



Deposited via The University of York.

White Rose Research Online URL for this paper:

<https://eprints.whiterose.ac.uk/id/eprint/167233/>

Version: Accepted Version

Article:

Gonzalez Alam, Tirso, Krieger-Redwood, Katya Melanie, Evans, Megan et al. (2021) Intrinsic Connectivity of Anterior Temporal Lobe Relates to Individual Differences in Semantic Retrieval for Landmarks. *Cortex; a journal devoted to the study of the nervous system and behavior*. pp. 76-91. ISSN: 1973-8102

<https://doi.org/10.1016/j.cortex.2020.10.007>

Reuse

This article is distributed under the terms of the Creative Commons Attribution-NonCommercial-NoDerivs (CC BY-NC-ND) licence. This licence only allows you to download this work and share it with others as long as you credit the authors, but you can't change the article in any way or use it commercially. More information and the full terms of the licence here: <https://creativecommons.org/licenses/>

Takedown

If you consider content in White Rose Research Online to be in breach of UK law, please notify us by emailing eprints@whiterose.ac.uk including the URL of the record and the reason for the withdrawal request.

Intrinsic Connectivity of Anterior Temporal Lobe Relates to Individual Differences in Semantic Retrieval for Landmarks

Tirso Rene del Jesus Gonzalez Alam, Katya Krieger-Redwood, Megan Evans, Grace E Rice,
Jonathan Smallwood and Elizabeth Jefferies

Abstract

Contemporary neuroscientific accounts suggest that ventral anterior temporal lobe (ATL) acts as a bilateral heteromodal semantic hub, which is particularly critical for the specific-level knowledge needed to recognise unique entities, such as familiar landmarks and faces. There may also be graded functional differences between left and right ATL, relating to effects of modality (linguistic versus non-linguistic) and category (e.g., knowledge of people and places). Individual differences in intrinsic connectivity from left and right ATL might be associated with variation in semantic categorisation performance across these categories and modalities. We recorded resting-state fMRI in 74 individuals and, in a separate session, examined semantic categorisation. People with greater connectivity between left and right ATL were more efficient at categorising landmarks (e.g. Eiffel Tower), especially when these were presented visually. In addition, participants who showed stronger connectivity from right than left ATL to medial occipital cortex showed more efficient semantic categorisation of landmarks regardless of modality of presentation. These results can be interpreted in terms of graded differences in the patterns of connectivity across left and right ATL, which give rise to a bilateral yet partially segregated semantic 'hub'. More specifically, right ATL connectivity supports the efficient semantic categorisation of landmarks.

Keywords: Hemispheric Differences, Modality, Anterior Temporal Lobe, fMRI, Intrinsic connectivity.

1. Introduction

Semantic cognition allows us to understand the world around us – including the meaning of words, objects, locations and people (Lambon Ralph et al., 2017; Patterson et al., 2007). Conceptual representations that underpin semantic performance across input modalities (e.g., words and pictures) and across different tasks are thought to be supported by the bilateral ventral anterior temporal lobes (ATL; Binney et al., 2010; Rice et al., 2015a, 2015b). Patients with semantic dementia have degraded conceptual knowledge that is associated with bilateral ATL atrophy, while other aspects of cognition remain largely intact (Lambon Ralph et al., 2017; Patterson et al., 2007). Semantic deficits following ATL damage are most pronounced for semantic tasks that probe specific-level knowledge – including knowledge of unique entities including people, such as Barack Obama, and landmarks, such as the Eiffel Tower (Rogers et al., 2015; Tranel, 2006; Tranel et al., 1997). An influential account of ATL function suggests that this region forms a semantic “hub” drawing together different features represented within ‘spokes’ (capturing visual, valence, language and auditory inputs) to form heteromodal concepts (Patterson et al., 2007). More detailed conceptual retrieval may be needed to identify unique entities and other specific concepts within this hub (Rogers et al., 2006); in line with this, unique entities activate ATL more strongly than more general-level concepts in neuroimaging studies of healthy participants (Gorno-Tempini and Price, 2001; Grabowski et al., 2001; Ross and Olson, 2012).

Neuropsychological and neuroimaging studies suggest that semantic representations draw on a *bilateral* hub, implemented across both left and right ATL (Ding et al., 2020; Lambon Ralph et al., 2017; Patterson et al., 2007). Severe semantic degradation follows bilateral ATL atrophy in semantic dementia; in contrast, patients with unilateral lesions following resection for temporal lobe epilepsy have measurable yet much milder semantic deficits (Rice et al., 2018a). This might reflect functional compensation by the intact ATL (Jung and Lambon Ralph, 2016). Neuroimaging studies with healthy participants have observed bilateral responses to semantic tasks in ATL (Visser et al., 2009), irrespective of whether words or pictures are presented (Bright et al., 2004; Tranel et al., 2005; Vandenberghe et al., 1996; Visser et al., 2012; Visser and Lambon Ralph, 2011). Inhibitory transcranial magnetic stimulation (TMS) delivered to either left or right ATL disrupts both picture and word-based semantic tasks, mimicking the pattern in semantic dementia (Pobric et al., 2010, 2007). Moreover, in line with expectations for a single semantic hub distributed across two hemispheres (cf. Schapiro et al., 2013), inhibitory TMS to left ATL leads to an increase in the

response within right ATL, suggesting the non-stimulated hemisphere may compensate for functional disruption within the stimulated hemisphere (Binney and Lambon Ralph, 2015; Jung and Lambon Ralph, 2016).

There is also evidence that left and right ATL are not functionally identical. The integration of different aspects of knowledge in ATL is thought to occur in a graded connectivity-dependent fashion (Bajada et al., 2019; Binney et al., 2012), with the most heteromodal responses in ventrolateral ATL (Lambon Ralph et al., 2017; Murphy et al., 2017; Visser et al., 2012). A degree of functional specialisation across the hemispheres might reflect differential white matter connections from visual, auditory-motor, social and emotional networks to left and right ATL (Papinutto et al., 2016; Rice et al., 2015a). Some studies have suggested a modality difference across the hemispheres – with left ATL showing stronger engagement for verbal tasks, and right ATL showing a preference for non-verbal tasks. Patients with semantic dementia who have relatively more left-sided or right-sided atrophy provide support for this suggestion (Gainotti, 2012): atrophy in right ATL correlates with difficulties on picture semantic tasks, while damage to left ATL is more strongly correlated with verbal semantic task performance (Butler et al., 2009; Mion et al., 2010). A variant of this modality view suggests that output modality is also important – damage to left ATL is particularly associated with problems in naming concepts (Lambon Ralph et al., 2001), and therefore with deficient lexical access from semantic knowledge, while right ATL is linked to poor object recognition (Damasio et al., 2004). These effects of modality across left and right ATL are most commonly reported in studies comparing semantic retrieval to people's names and faces (Gainotti, 2013, 2007; Gainotti and Marra, 2011; Luzzi et al., 2017; Snowden et al., 2017, 2012): for example, Snowden et al. (2004) found that patients with more left-lateralised atrophy had greater impairment for people's names, while patients with more right-sided atrophy had greater difficulty on semantic tasks employing faces. Given that multiple neuropsychological studies have found hemispheric differences in ATL when contrasting famous people's names and faces, individual differences in connectivity from left and right ATL in healthy participants might also relate to these aspects of semantic cognition (see below; less is currently known about modality effects for the landmark category).

An alternative account suggests that hemispheric specialisation in left and right ATL reflects semantic category, not (only) input modality – by this view, right ATL has been argued to play a larger role than left ATL in understanding social concepts and retrieving conceptual information about specific people (Zahn et al., 2007). Patients with damage to right ATL

often have particular difficulties recognising faces, but there is an ongoing debate about whether these difficulties reflect impairment for faces per se (i.e. difficulty when the task involves both social stimuli and picture inputs) or a wider problem with social concepts (Gainotti, 2013; Gorno-Tempini et al., 1998; Olson et al., 2013, 2007; Ross and Olson, 2010).

In addition, a few neuroimaging studies have contrasted knowledge of famous faces and names with knowledge of landmarks (since both of these categories comprise unique entities): this contrast reveals common activation for both faces and landmarks in left ATL (Gorno-Tempini and Price, 2001; Grabowski et al., 2001; Wang et al., 2016), and weaker engagement of right ATL across both categories. A recent fMRI study (Rice et al., 2018b) directly compared the neural response in ATL during semantic decisions about specific entities that were social (people) and non-social (landmarks). The social and non-social stimuli were presented as both words (i.e., people's names) and as pictures (i.e., faces). Both the left and right ventral ATL responded regardless of the modality or category of semantic information, although an additional bilateral region in the ATL, extending towards the temporal pole, showed stronger activation to people vs. landmarks. Similarly, a meta-analysis of 97 functional neuroimaging studies (Rice et al., 2015b) confirmed that both left and right ATL were activated across verbal and non-verbal stimuli, and social and non-social tasks. Studies involving word retrieval were more likely to report unilateral left ATL activation, while social semantic studies were more likely to observe bilateral ATL activation.

Rice and colleagues (2015b) suggested that subtle functional differences between left and right ATL are likely to reflect differential connectivity to 'spoke' systems – for example, stronger connectivity between right ATL and visual regions, or between left ATL and language regions. In this extension of the "graded hub account", the bilateral semantic store shows some degree of differentiation between left and right ATL, such that distinct patterns of connectivity can explain modality effects (for example, differences between faces and names). Semantic retrieval for different categories is also thought to draw disproportionately on particular feature types – for example, visual textures and movement are critical to the animal category, while action features and hand shape are important for tools (Fernandino et al., 2016; Ishibashi et al., 2016; Liljeström et al., 2008; Mollo et al., 2018; Moss et al., 2005, 1998; Rogers et al., 2005). Consequently, this type of account is potentially able to accommodate differences in the contributions of left and right ATL to distinct semantic categories, such as people versus landmarks, as well as effects of modality. In a recent study (Gonzalez Alam et al., 2019), left ATL was more connected with other sites implicated in

semantic cognition (e.g. left inferior frontal gyrus, posterior middle and inferior temporal cortex), while right ATL was more connected to visual cortex and default mode network regions, including angular gyrus and dorsomedial prefrontal cortex. Despite these differences, ATL had the most symmetrical connections within the semantic network (i.e. the highest correlations between connectivity patterns generated from left and right-hemisphere seeds), consistent with the bilateral hub theory.

Individual differences in patterns of connectivity from left and right ATL might differentially relate to the efficiency of semantic decisions about people and landmarks, presented as words and pictures. Gonzalez Alam et al. (2019) failed to observe any behavioural correlates of hemispheric differences in ATL connectivity; however, this previous study did not use tasks designed to maximise the involvement of this brain area (i.e. specific-level concepts). Studies show that individual differences between participants in the strength of intrinsic connectivity, defined according to time-series correlations in resting-state fMRI, are associated with variation in cognitive performance (Cole et al., 2014; Smith et al., 2009; Van Dijk et al., 2010), including semantic cognition (Evans et al., 2020; Gonzalez Alam et al., 2018; Mollo et al., 2016; Poerio et al., 2017; Vatansever et al., 2017; Zhang et al., 2019). Hemispheric differences in intrinsic connectivity across individuals have already been linked to semantic and spatial tasks (Gonzalez Alam et al., 2019; Sormaz et al., 2017; although these prior studies did not find associations with ATL connectivity). Individual differences in the connectivity of ATL have also been associated with semantic processing, although these studies did not examine hemispheric differences (Mollo et al., 2016; Vatansever et al., 2017).

To address this gap in the literature, the current study acquired resting-state fMRI from 74 participants, who completed semantic decisions about specific people and landmarks, presented as written words and pictures (using the stimuli from Rice et al., 2018b) in a separate testing session following the scan. We then assessed relationships between connectivity and behavioural performance – with particular focus on whether right vs. left ATL connectivity would predict performance on these different categories presented as pictures vs. words.

2. Methods

This study includes analysis of intrinsic connectivity in a sample of participants who performed a resting-state scan and behavioural testing in two separate sessions. We

determined our sample size based on participant availability (i.e., tested as many of the participants with resting-state data as were willing), and report all data exclusions, all inclusion/exclusion criteria, whether inclusion/exclusion criteria were established prior to data analysis, all manipulations, and all measures in the study. This study was not pre-registered in a time-stamped, institutional registry prior to the research being conducted.

2.1. Participants

This study was approved by the local research ethics committees. Participants who had previously received a resting-state scan were invited to return to the lab for behavioural testing. The recruited sample consisted of 83 participants (19 male, 64 female, mean age=19.69, range=18-26). Two participants were removed before pre-processing due to missing resting-state scans, and a further three due to not having full brain coverage. Another two were excluded during pre-processing because they exceeded our quality assessment measures of (i) motion greater than 0.3mm, (ii) invalid scans greater than 20%; and/or (iii) global mean signal change greater than $z=2$. Finally, two more participants were excluded because they performed at least one behavioural task at chance level, leaving us with a final sample size of 74 participants recruited from undergraduate and postgraduate students at the University of York. All participants were right handed, native English speakers with normal/corrected vision. During scanning, we also excluded participants with a history of psychiatric or neurological illness, severe claustrophobia, drug use that could alter cognitive functioning, and pregnancy. These inclusion and exclusion criteria were established during the study design and prior to any data being collected. All volunteers provided written informed consent and were either paid or given course credit for their participation.

2.2. Procedure

In the initial neuroimaging session, we acquired structural MRI images and a resting-state scan during which participants were instructed to keep their eyes open and focus on a fixation cross. We invited participants back for a behavioural session involving five tasks. The duration of the full testing session was approximately 1.5 hours. The task used in the current

study was towards the end of this session. To control for order effects, each participant completed the tasks in the same order.

2.3. Task

We adapted a task from Rice et al. (2018b). Participants were presented with different categories of stimuli (animals, landmarks and people) as either images or written words (in the original task the latter were presented as spoken words). They had to judge whether the stimuli were European or non-European. The faces were presented on a relatively plain background, and the landmarks and animals were the central object within a naturalistic image that included the immediate context. Participants were also presented with a non-semantic perceptual control condition, in which they were shown a scrambled image (generated by taking the pixels from the images in the other conditions and randomising their location so they were devoid of meaning) and asked to judge whether it was presented higher or lower on the screen. Examples of the stimuli in each condition are shown in Figure 1.

Stimuli were taken from Rice et al. (2018b) and reduced to only include trials with 85% accuracy or above in Rice's data, providing 60 stimuli per category. Blocks consisted of 30 trials each (480 trials in total), all drawn from the same category and modality, with random assignment of stimuli to blocks. There were sixteen blocks (four conditions by two modalities; with each combination presented twice). The blocks were presented in four possible sequences, to which participants were randomly assigned.

Each trial lasted 3s, consisting of a 500ms fixation cross followed by 2500ms stimulus presentation (see Figure 1). Participants indicated their response using the '1' key on a computer keyboard for European/higher location and '2' for non-European/lower location. Before the task commenced, an instruction slide was presented which remained on screen until the participant indicated they were ready to begin via key press. At the beginning of each block, a cue screen indicating the condition was presented for 500ms. Every four blocks participants were presented with a rest screen until they indicated they were ready to continue via key press. Both response time (RT) and accuracy were recorded, and an efficiency score was calculated for each participant in each condition by dividing median response times by accuracy (note: in brain analyses, this efficiency score was inverted to aid the interpretation of the results, such that a higher score corresponded to better performance). This approach allowed us to control for speed-accuracy trade-offs when assessing associations with intrinsic

connectivity, and avoid the inflation of Type 1 errors that would result from running parallel analyses for accuracy and RT separately. Efficiency scores are widely used in contexts in which it is necessary to combine accuracy and RT (Draheim et al., 2016; Jackson et al., 2015; Vandierendonck, 2017). The duration of the whole task was 15-20 minutes. The task was implemented in E-prime 2.0. The code and source materials of the task are publicly accessible on the following OSF repository: <https://osf.io/m85rc/>.

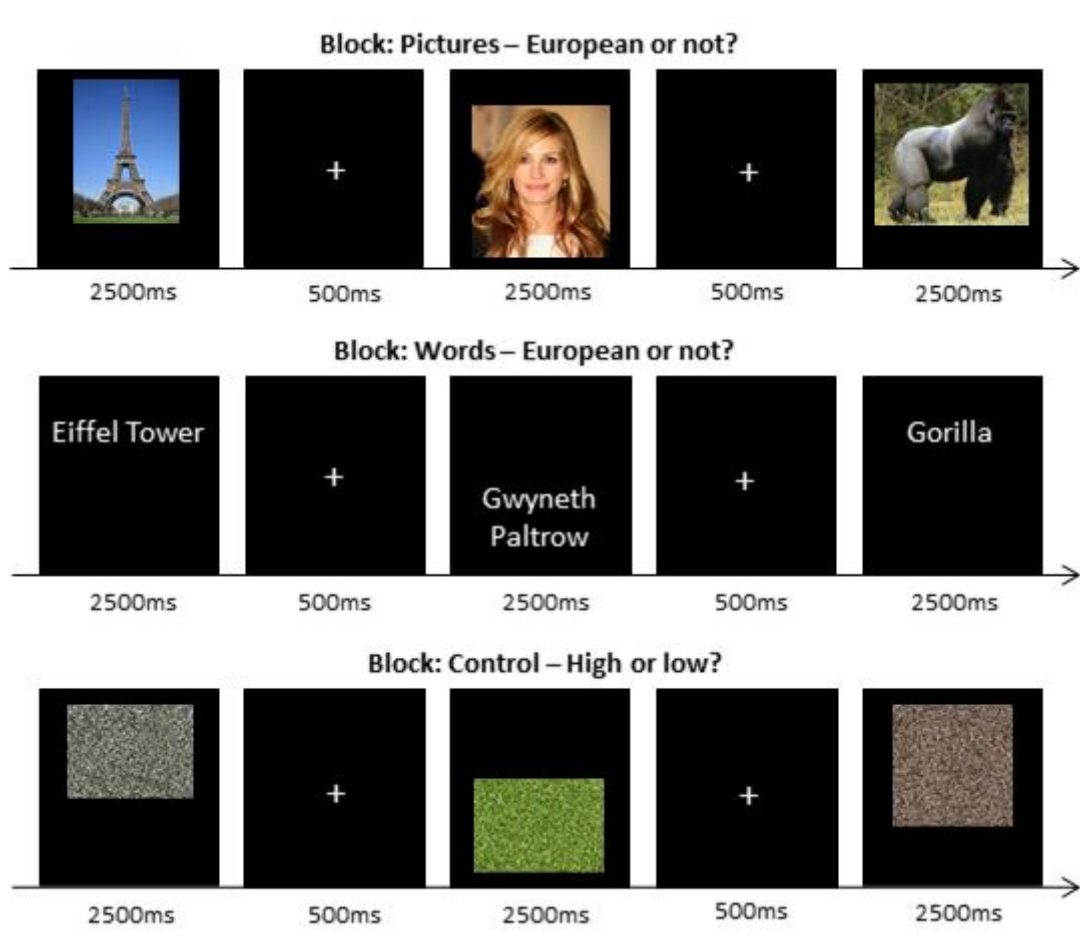


Figure 1. Example stimuli and trial structure for each condition in the semantic representation task and non-semantic control task. This is a simplification of the actual structure of the task, where the stimuli were not only blocked by modality of presentation, but also by category of stimuli (i.e. “pictures of landmarks” would be a block).

2.4. Neuroimaging

2.4.1. *MRI data acquisition*

MRI data was acquired using a 3T GE HDx Excite Magnetic Resonance Imaging (MRI) system utilising an eight-channel phased array head coil tuned to 127.4 MHz, at the York

Neuroimaging Centre, University of York. Structural MRI acquisition in all participants was based on a T1-weighted 3D fast spoiled gradient echo sequence (TR = 7.8s, TE = minimum full, flip angle = 20°, matrix size = 256 × 256, 176 slices, voxel size = 1.13 × 1.13 × 1 mm). A nine-minute resting state fMRI scan was carried out using single-shot 2D gradient-echo-planar imaging (TR = 3s, TE = minimum full, flip angle = 90°, matrix size = 64 × 64, 60 slices, voxel size = 3 × 3 × 3 mm³, 180 volumes). Participants were asked to passively view a fixation cross and not to think of anything in particular during the resting-state scan. A FLAIR scan with the same orientation as the functional scans was collected to improve co-registration between subject-specific structural and functional scans.

2.4.2. *Pre-Processing*

All pre-processing of resting-state data was performed using the CONN functional connectivity toolbox V.18a (<http://www.nitrc.org/projects/conn>; Whitfield-Gabrieli & Nieto-Castanon, 2012). MRI data pre-processing and statistical analyses were carried out using the SPM software package (Version 12.0), based on the MATLAB platform (Version 17a) implemented in CONN. For pre-processing, functional volumes were slice-time (bottom-up, interleaved) and motion-corrected, skull-stripped and co-registered to the high-resolution structural image, spatially normalized to the Montreal Neurological Institute (MNI) space using the unified-segmentation algorithm, smoothed with a 6 mm FWHM Gaussian kernel, and band-passed filtered (0.008 – 0.09 Hz) to reduce low-frequency drift and noise effects. A pre-processing pipeline of nuisance regression included motion (twelve parameters: the six translation and rotation parameters and their temporal derivatives), scrubbing (all outlier volumes were identified through the artifact detection algorithm included in CONN, with conservative settings: scans for each participant were flagged as outliers based on a composite metric with parameters set to scan-by-scan change in global signal z-value threshold = 3, subject motion threshold = 5mm, differential motion and composite motion exceeding 95% percentile in the normative sample) and CompCor components (the first five) attributable to the signal from white matter and CSF (Behzadi et al., 2007), as well as a linear

detrending term, eliminating the need for global signal normalization (Chai et al., 2012; Murphy et al., 2009).

2.4.3. *ROI Selection*

We used a left ventral ATL site identified by Rice et al. (2018b) as showing peak activation for semantic > non-semantic contrasts across eight studies using distortion-corrected fMRI (MNI coordinates -41, -15, -31). Since there is good evidence of bilateral engagement of ATL in semantic cognition, and Rice et al. (2018b) identified a right ATL functional peak (MNI 44, -11, -36), we also included this seed in our investigation. We created ROIs by placing a binarised spherical mask with a radius of 3mm at these MNI coordinates. The BOLD time series extracted for each seed region was an average for all voxels making up the sphere.

2.4.4. *Resting-State fMRI Analysis*

This analysis examined individual differences in the connectivity of left and right ATL to the rest of the brain, measured through resting-state fMRI, and related these differences to behavioural efficiency scores on semantic tasks (measured outside the scanner in a separate session). In a first-level analysis, we extracted the time series from each of the ROIs for each participant. We computed the seed to voxel correlations for each of our seeds, removing the nuisance regressors detailed in section 2.4.2. At the group level, our analysis focused on associations between hemispheric similarities and/or differences in the connectivity of ATL and behavioural effects of the category of the stimuli and the modality of presentation. We entered into a GLM the mean-centred efficiency scores (with outliers +/-2.5 SD imputed to +/-2.5) of five task conditions (excluding the Animal Verbal condition, and the non-semantic Control condition, due to performance levels at chance and at ceiling, respectively), together with a nuisance regressor containing mean motion (measured in framewise displacement) for each participant as EVs.

We performed functional connectivity weighted GLM seed-to-voxel analyses convolved with a canonical haemodynamic response function (HRF). There were four analyses: two models for the single seeds (left ATL, right ATL; **presented in Supplementary Materials**); one model examining connectivity across left and right ATL (a seed region that encompassed both

hemispheres); and finally one model that examined the difference between left and right ATL (examining left versus right functional peaks). We applied Bonferroni correction to the FWE values resulting from two-sided t-tests in the models to determine significant clusters (correcting for these four models). Besides the mean group connectivity for each seed, we defined the following contrasts of interest: category (People > Landmarks and vice-versa), modality (Verbal > Visual and vice-versa), modality by category interaction (the effect of modality for people versus landmarks) and the main effects for the five tasks conditions (i.e. Verbal Landmark, Verbal People, Visual Landmark, Visual People and Visual Animals).

At the group-level, analyses were carried out using CONN with cluster correction (with results reaching $p < .013$ considered to be significant, corresponding to $p < .05$ following Bonferroni correction to control for the four models we ran; see above), and a threshold of $z=3.1$ (p -FWE=0.001) to define contiguous clusters (Eklund et al., 2016). This analysis included the behavioural regressors described above (as mean-centred inverse efficiency scores for each task condition) to evaluate whether performance correlated with individual differences in intrinsic connectivity. The connectivity maps resulting from these analyses were uploaded to Neurovault (Gorgolewski et al., 2015, URL:

<https://neurovault.org/collections/5687/>). The conditions of our ethics approval do not permit public archiving of the data and code supporting this study. Readers seeking access to this data should contact the lead author, Tirso RJ Gonzalez Alam, the PI Professor Beth Jefferies, or the local ethics committee at the Department of Psychology and York Neuroimaging Centre, University of York. Access will be granted to named individuals in accordance with ethical procedures governing the reuse of sensitive data. Specifically, the following conditions must be met to obtain access to the data: approval by the Department of Psychology and York Neuroimaging Research Ethics Committees and a suitable legal basis for the release of the data under GDPR. As a confirmatory analysis, to verify that the results were not dependent on an arbitrary significance threshold, we carried out non-parametric permutation testing as implemented in CONN for each significant result that survived Bonferroni correction. All clusters were replicated by permutation testing.

In order to interpret the results that survived Bonferroni correction, we used the significant clusters as binarised masks and extracted the global-scaled mean connectivity for each seed per participant to each significant cluster using REX implemented in CONN (Whitfield-Gabrieli & Nieto-Castanon, 2012). These values were then related to each participant's mean-centred inverse efficiency score for the relevant EV, and plotted as scatterplots using Seaborn

in Python 2.7, colour coded so that red scatterplots show connectivity from the left ATL seed and blue scatterplots show connectivity from the right ATL seeds.

2.4.5. Control Analysis

Due to the functional heterogeneity of ATL (Rice et al., 2015a), the exact seed location can have an impact on the results. Since in a previous study we found significantly different patterns of cross-hemisphere connectivity in ATL depending on whether sign-flipping or functional peaks were used to define the right-hemisphere seed (Gonzalez Alam et al., 2019), we carried out a control analysis using homotopic left and right ATL seeds.

For this control analysis, we generated a right-hemisphere sphere from coordinates for the left ventral ATL peak identified by Rice et al. (2018b), flipping the sign of the x-coordinate in MNI space from negative to positive (MNI coordinates 41, -15, -31). Consequently, in this analysis, left and right ATL sites were anatomically equivalent, while in our main analysis, we used functional peaks in left and right ATL which were in similar but non-identical locations (see supplementary Figure S3 for the relative position of the right ATL seeds). We performed the same GLM with this homotopic sign-flipped right-hemisphere seed as with the functionally-defined seed. We then binarised the significant results obtained from the functionally-defined seed in our main analysis and asked whether the same patterns could be observed using the homotopic sign-flipped seeds: we extracted the connectivity of the left functional and right sign-flipped seeds, and regressed these patterns of connectivity against the behavioural contrast that gave rise to each neuroimaging effect. This allowed us to verify whether the effects we report below were dependent on seed selection. To anticipate, we found the results from our main analysis were replicated.

3. Results

3.1. Behavioural Results

Figure 2 shows the average median reaction time, accuracy and efficiency scores in each condition of the semantic task adapted from Rice et al. (2018b). A two-way repeated measures ANOVA on reaction time data with category and modality as factors revealed no main effect of modality, a significant main effect of category and a category by modality

interaction [Category: $F(2,144) = 56.07, p < .001$; Interaction: $F(2,144) = 69.1, p < .001$]. Post-hoc tests with Bonferroni correction showed no difference between people and landmarks, but significant differences between animals and all other conditions, with participants responding more slowly on animal trials ($p < .001$). Post-hoc testing with Bonferroni correction also confirmed the interaction was driven by slower performance for verbal than visual animal judgements ($p < .001$). The same analysis for accuracy found significant effects of category, modality and a category by modality interaction [Category: $F(2,144) = 174.39, p < .001$; Modality: $F(2,144) = 487.39, p < .001$; Interaction: $F(2,144) = 41116.11, p < .001$]. Post-hoc tests with Bonferroni correction revealed that participants showed equivalent accuracy for landmark and people judgements, but both of these significantly differed from animal judgements, where participants made more errors ($p < .001$). Likewise, participants were significantly less accurate in verbal than picture judgements ($p < .001$). The interaction was driven by participants being significantly less accurate for verbal than visual judgements about animals ($p < .001$).

Speed and accuracy may be traded off in different ways across tasks and individuals. To address this issue we calculated response efficiency scores, computing reaction time divided by accuracy to characterise global performance (inverted for neuroimaging analyses, so that high scores reflect good performance in the scatterplots depicted in Figures 4 – 6 and supplementary figures: these figures depict each participant's efficiency z-scored relative to the group performance in each condition). A two-way repeated measures ANOVA of participants' efficiency scores with Greenhouse-Geisser correction using category and modality as factors showed significant effects of category, modality and an interaction using this response efficiency measure [Category: $F(1.7,122.6) = 63.22, p < .001$; Modality: $F(1,72) = 136.08, p < .001$; Interaction: $F(1.8,130) = 478.47, p < .001$]. Post-hoc tests once again found no difference between judgements about landmarks and people, plus significantly better performance in both of these conditions compared with animal trials ($p < .001$). Participants performed less efficiently in verbal than visual judgements ($p < .001$), while the interaction was driven by participants being less efficient in verbal than visual judgements about animals ($p < .001$).

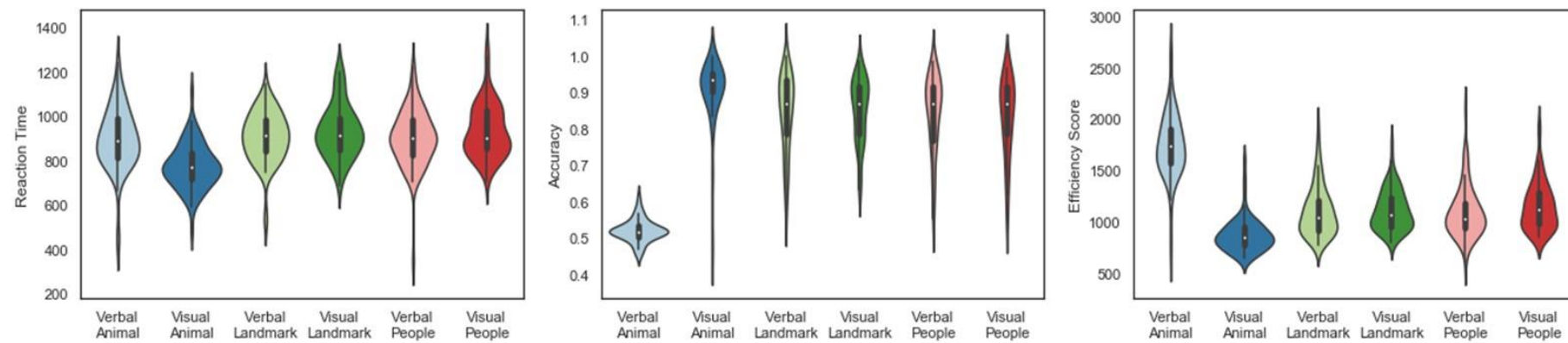


Figure 2. Violin plots depicting the average median reaction time (milliseconds), accuracy (proportion correct) and efficiency scores (reaction time divided by accuracy) for the semantic categorisation task. The width of each bar shows the frequency of scores for the values plotted.

3.2. Mean connectivity of left and right ATL (without behavioural regressors)

We examined the single seed mean connectivity for each ATL, as well as mean connectivity from both seeds combined, and differential left vs. right connectivity. The results are shown in Figure 3. The left ATL seed showed a pattern of bilateral functional connectivity overlapping with the semantic cognition network (shown for reference in the top row) in the LH, including medial and lateral aspects of the temporal lobe extending posteriorly to the angular gyrus bilaterally, as well as parts of the inferior frontal gyrus (extending more anteriorly in the LH) and central sulcus, posterior cingulate cortex and frontal poles (Figure 3, second row). The right ATL seed showed positive connectivity to ventral aspects of the left temporal lobe and right temporal pole. It also showed positive connectivity to left angular gyrus, inferior frontal and posterior middle temporal gyri, frontal pole and medial aspects of the temporal lobe, plus weak connectivity to bilateral occipital lobes. Unlike left ATL, the RH seed did not show connectivity to the central sulcus, but it did to bilateral superior frontal gyrus and medial orbitofrontal cortex extending posteriorly to the posterior cingulate cortex (Figure 3, third row). This pattern is similar to that described by Gonzalez Alam et al. (2019). An analysis giving equal weight to both left and right ATL seeds captured this similarity between the maps, including strong connectivity in bilateral temporal regions extending into angular gyrus, as well as inferior and superior frontal gyri, posterior cingulate and orbitofrontal cortex, with common weak connectivity in medial occipital cortex (Figure 3, fourth row). Significant differences between the left and right ATL included the left ATL seed showing stronger connectivity with left dorsal ATL and bilateral dorsal central sulcus, while the right ATL seed showed stronger connectivity with left middle frontal gyrus, orbitofrontal and ATL (Figure 3, bottom row).

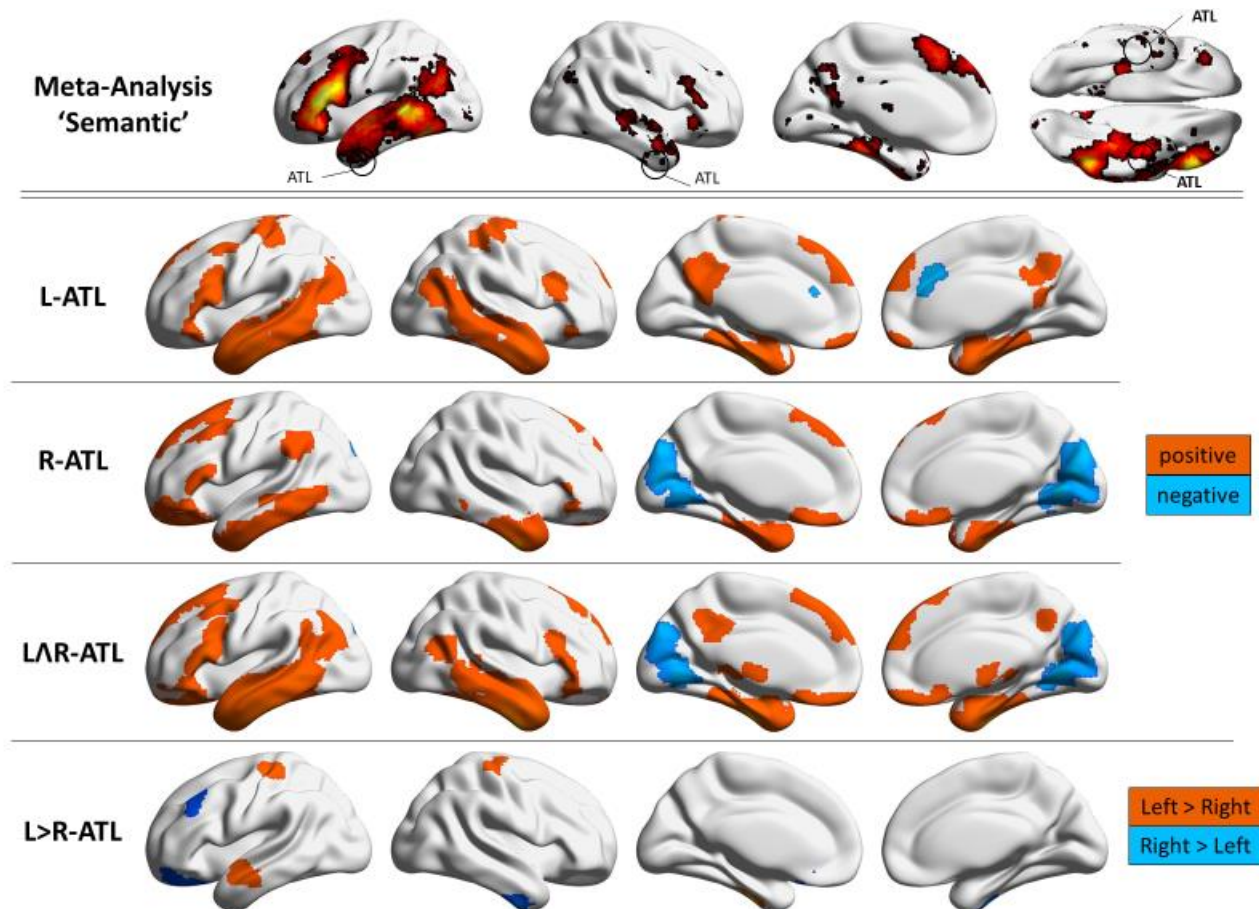


Figure 3. The top row depicts a term-based meta-analysis of the term ‘Semantic’ in Neurosynth. The four following rows show resting-state connectivity for left and right anterior temporal lobe, plus their common and differential connectivity. For the single seeds and mean left plus right ATL maps, the warm and cool colours represent positive and negative patterns of connectivity respectively, while for the difference analysis the warm and cool colours represent left and right connectivity respectively. The group maps are thresholded at $z = 3.1$, $p = 0.05$.

3.3. Behavioural consequences of ATL connectivity – overview of analysis aims

We performed whole brain resting-state functional connectivity analysis using behavioural performance in five conditions of our semantic representation task as covariates, to probe for possible associations between seed connectivity and categorisation efficiency. We did not include the verbal animal condition due to chance-level performance. For each significant result found using a cluster-forming threshold of $z = 3.1$, we ran non-parametric analysis using CONN to confirm whether the result was robust irrespective of this particular cluster-forming threshold. All results presented in this section were replicated across these analyses. Table 1 presents a full list of significant results, after Bonferroni correction for 4 comparisons, as well as which results are significant using non-parametric statistics. In the

following sections, we first present the results of analyses for combined left and right ATL seeds (i.e. mean connectivity across both hemispheres), followed by analyses of differences between left and right ATL connectivity. Behavioural associations for the single seeds (i.e. for left and right ATL seeded separately) were captured by the results of the combined analyses reported below. These results are reported in the supplementary materials, in Figures S1 and S2.

The results converged on two main findings: (i) the strength of connectivity between right ATL and medial occipital cortex was associated with efficient performance on landmarks trials, regardless of modality; and (ii), the strength of connectivity between left and right ATLs (especially stronger bilateral ATL connectivity) was linked to better performance on landmark trials in the picture modality. We show the overlap of different results relating to this latter effect in Figure 7.

Seed	Contrast	Cluster	Vox.	p-FWE	Non-param. p	x	y	z
Single Seeds								
L-ATL	Visual > Verbal	R-ATL	242	<.001	.035	48	10	-44
	Landmark							
L-ATL	Interaction	R-ATL	169	.032	>.05	40	14	-46
R-ATL	Visual > Verbal	L-TP	575	<.001	.003	-42	-4	-34
	Landmark	R-TP	175	.012	>.05	38	12	-42
R-ATL	Visual Landmark	R-TP	158	.042	>.05	38	12	-42
Combined Results								
L and R ATL	Interaction	R-TP	186	.02	.047	48	6	-40
L and R ATL	Visual Landmark	R-TP	292	<.001	.02	48	10	-36
L and R ATL	Visual > Verbal	L-ATL	649	<.001	.002	-42	-4	-48
L and R ATL	Landmark	R-ATL	539	<.001	.004	38	12	-44
R > L ATL	Main Landmark	L-OP	187	.016	> .05	-12	-100	8

Table 1. Summary of significant results. Note. The p-FWE values are Bonferroni-corrected for four multiple comparisons. The “Non-param. p” column reports the significance value (p-FWE) obtained using non-parametric statistics (5,000 simulations) as implemented in CONN. L = Left; R = Right; ATL = Anterior Temporal Lobe; TP = Temporal Pole; OP = Occipital Pole

3.4 Mean connectivity across left and right ATL and associations with behaviour

The mean connectivity of left and right ATL was significantly associated with three behavioural results. First, we found a significant interaction between modality and category (see Figure 4). Stronger connectivity from the combined left and right ATL seed to a more anterior right-lateralised cluster in the temporal pole was associated with better performance in the visual than verbal modality for landmarks, **whilst this effect was not observed for trials involving people knowledge**. We also found two significant results for the landmarks task, consistent with this interaction. Connectivity of the bilateral seed to a bilateral cluster encompassing left and right ATL, extending to the temporal pole, was associated with better visual than verbal categorisation for landmarks (see Figure 5, top panel). People who were better at categorising visual landmarks overall also had stronger connectivity between the bilateral ATL seed and right temporal pole (Figure 5, bottom panel). In order to confirm that these findings reflected cross-hemispheric connectivity, we plotted the results for ATL seed regions within left and right hemisphere separately. These plots show that left and right-lateralised parts of the seed were both associated with better categorisation for the picture landmark condition. All of these results taken together suggest that stronger connectivity to bilateral temporal pole is seen in participants who show better categorisation of landmarks when these are presented as pictures as opposed to words.

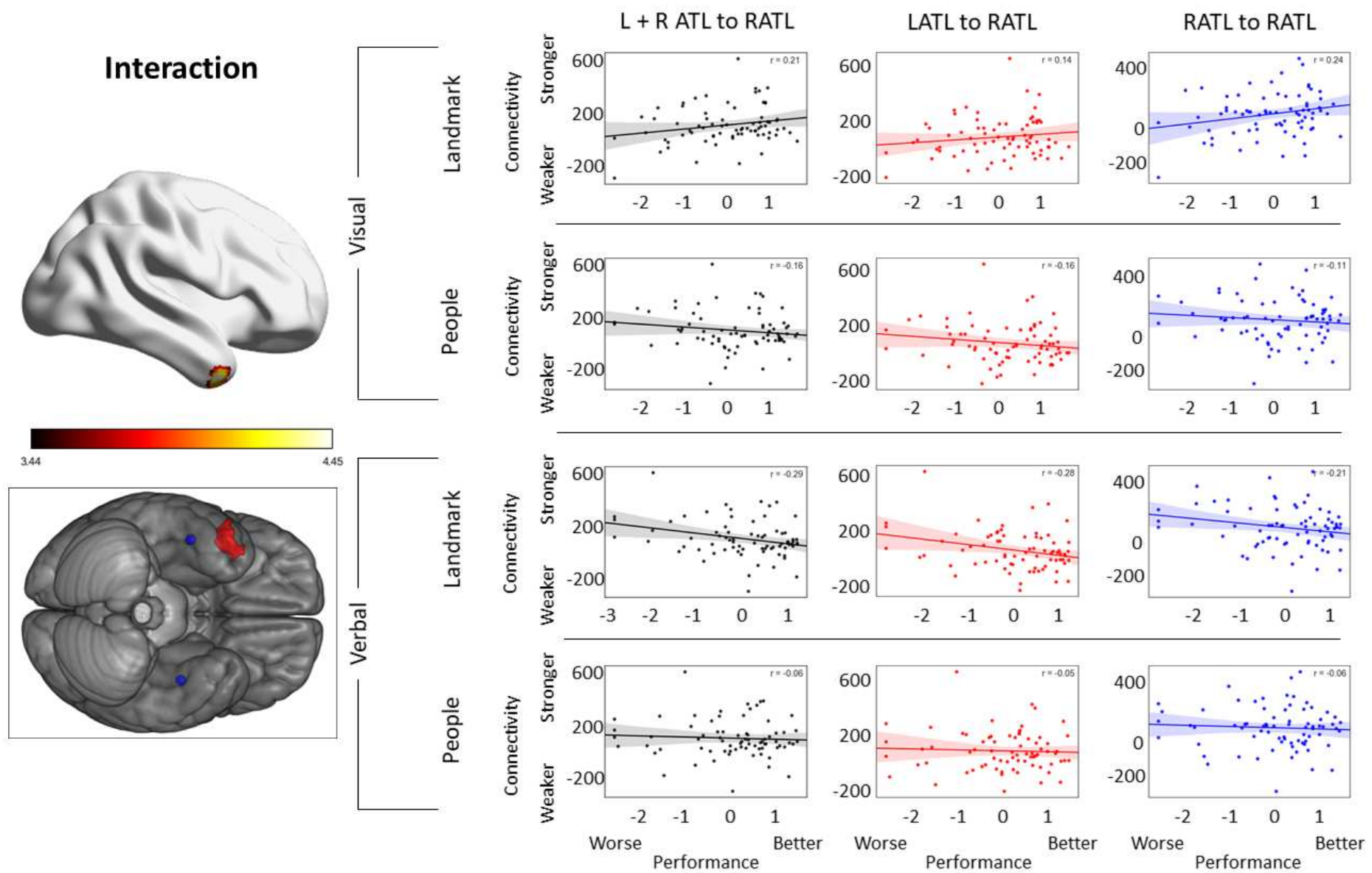


Figure 4. The connectivity between a right temporal pole cluster and the bilateral ventral ATL seed (defined using distinct functional peaks in both hemispheres) was associated with a modality by category interaction ($Z=3.1$, $p=.05$, Bonferroni-corrected for 4 models). The scatterplots depict the mean-centred efficiency scores (given in z-scores), plotted as a function of the normalised functional connectivity (i.e. scaled to the global mean) between the right temporal pole cluster depicted in the figure and seed regions comprising both left and right ATL functionally-defined seeds (black), left functionally-defined ATL (red), and right functionally-defined ATL (blue). The seeds have been plotted alongside the cluster on a separate brain image to depict their relative position. All units are given in z-scores.

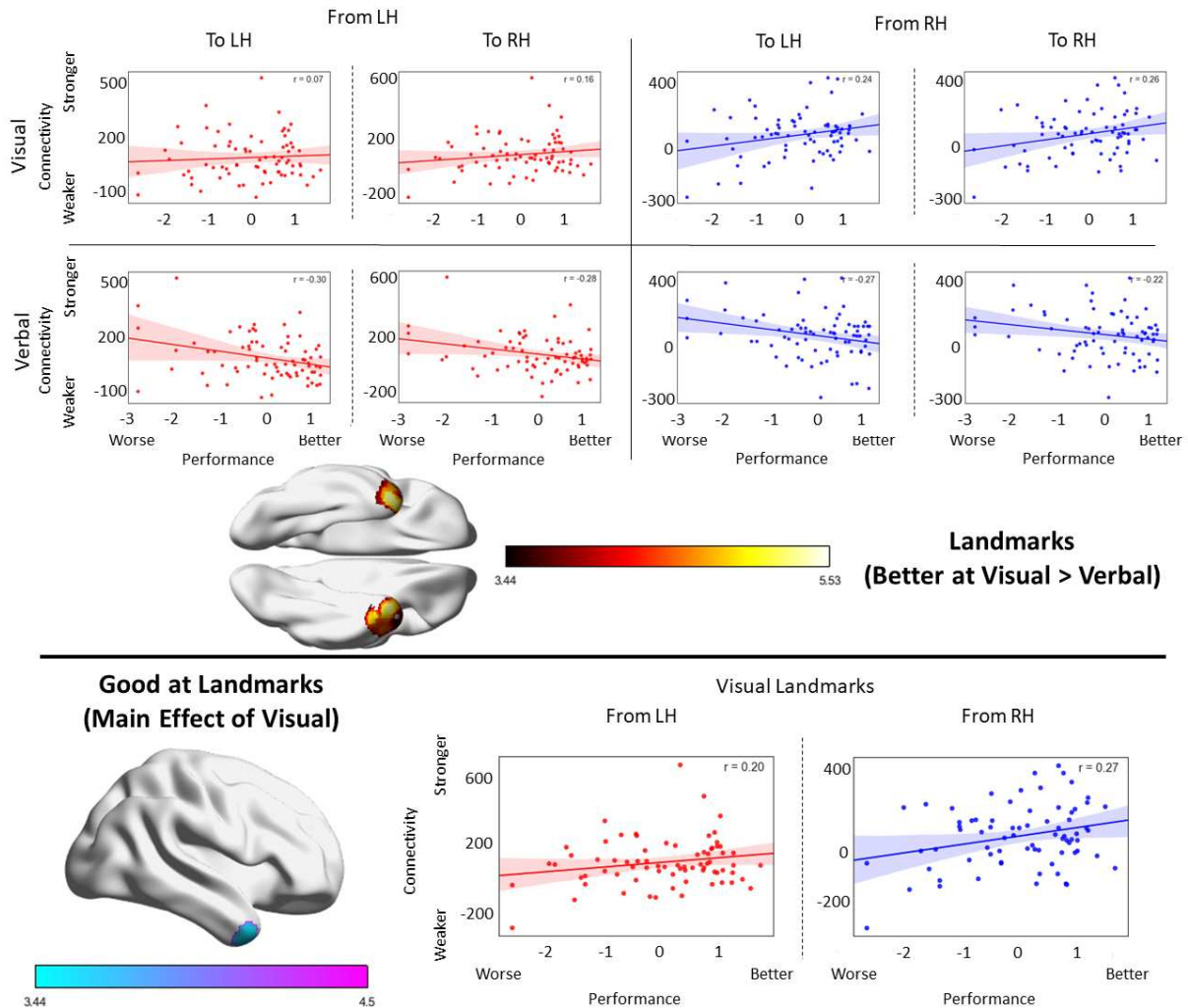


Figure 5. Top panel: Bilateral temporal pole clusters whose connectivity to bilateral left and right ventral ATL was significantly associated with being better at visual relative to verbal landmark judgements. Bottom panel: a right temporal pole cluster whose connectivity to bilateral left and right ventral ATL was significantly associated with the main effect of being good at visual landmarks (both results are thresholded at $Z=3.1$, $p=.05$, Bonferroni-corrected for 4 models). The scatterplots depict the mean-centred efficiency scores in the relevant condition (given in z-scores) plotted as a function of the normalised functional connectivity (i.e. scaled to the global mean) from both left ATL (red) and right ATL (blue) functional peaks to the clusters depicted in the figure. All units are given in z-scores.

3.5. Differential ATL connectivity between hemispheres and associations with behaviour

In a second set of analyses, we examined whether differences in connectivity between left and right ATL related to semantic performance. A whole-brain difference analysis contrasting left ATL over right ATL revealed a significant result located in medial occipital lobe / occipital pole, relating to performance for landmarks, regardless of modality (Figure 6).

Participants with more right than left ATL connectivity to this occipital pole cluster showed better performance for landmarks.

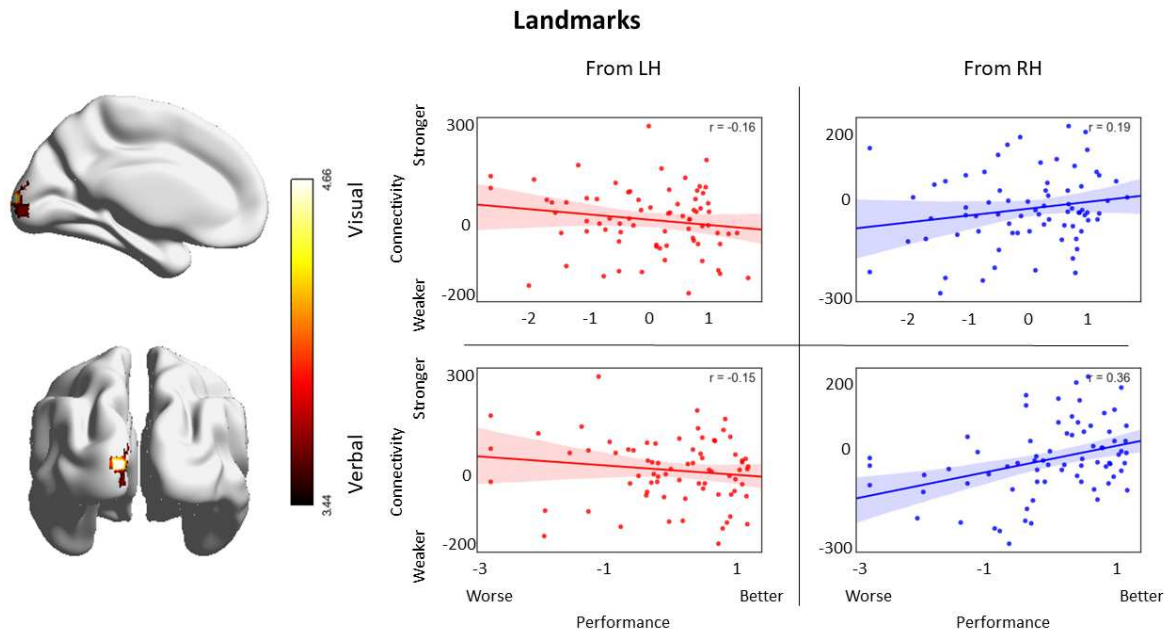


Figure 6. A polar occipital cluster whose differential connectivity to left ATL versus functionally-defined right ATL was significantly associated with landmarks performance ($Z=3.1$, $p=.05$, Bonferroni-corrected for 4 models). The scatterplots depict the mean-centred efficiency scores in the relevant condition (given in z-scores) plotted as a function of the normalised functional connectivity (i.e. scaled to the global mean) for left ATL (red) and right functionally-defined ATL (blue) to the cluster depicted in the figure.

3.6. Control analysis using homotopic seeds in same anatomical location across left and right ATL

In the main analysis above, we used functionally-defined left and right ventral ATL sites (i.e. sites in each hemisphere that showed peak activation for semantic versus non-semantic contrasts). As these sites were in similar but not identical locations in the two hemispheres, we performed a control analysis, which compared the left hemisphere functional peak with a right-hemisphere homotopic seed, generated by flipping the sign of the x coordinate in MNI space from negative to positive. Supplementary figure S3 provides a comparison of the location of the homotopic and functionally-defined right-hemisphere seeds: these two sites are shown to be adjacent but largely non-overlapping. The connectivity of this alternative

homotopic right ATL seed was similar yet distinct from the functional seed used in the main analysis (see Supplementary Figure S4).

Our key motivation was to establish if behavioural associations identified through whole-brain analysis of the functional seeds (reported above) could still be observed using the homotopic right ATL seed. We performed a series of ROI analyses, using the clusters obtained in our main analysis (Figures 4-6) as a mask. We extracted the average connectivity across the voxels in these masks for the homotopic left and right ATL seeds, scaled to the global mean for each participant using REX software implemented in CONN. A simple linear regression was calculated for each effect, predicting behavioural performance from the connectivity of these seeds to each relevant cluster. For more complex behavioural effects, repeated-measures ANOVA was used to capture interacting effects of modality and category, with the relevant pattern of connectivity included as a predictor.

The results of these analyses replicated the pattern we obtained using the functionally-defined right ATL seed. The regression for the interaction effect (presented in Figure 4) was significant ($F(1,72) = 9.189, p = .003$). The regression for the visual > verbal landmark effect (Figure 5, top row) was significant for both the left cluster ($F(1,72) = 6.190, p = .015$), with an R^2 of .079, and its right counterpart ($F(1,72) = 6.394, p = .013$), with an R^2 of .083. The regression for the main effect of visual landmarks (Figure 5, bottom row) was also significant ($F(1,72) = 6.394, p = .013$), with an R^2 of .083. Finally, the regression for the left > right ATL main effect of landmarks result was significant ($F(1,72) = 4.659, p = .034$), with an R^2 of .061. These findings show that our whole-brain results above do not solely reflect anatomical differences in seed location across left and right hemispheres.

3.7 Summary of results

We found that higher connectivity between left and right ATL is associated with better categorisation of landmarks, especially for the visual modality. There was a main effect reflecting an association between stronger connectivity and better performance on the picture-based landmark condition, a significant effect of modality for landmarks and an interaction between category and modality that all reflected the same pattern. We summarise the spatial distribution of these effects and their overlap in Figure 7. Distinct from these effects, greater right than left hemisphere connectivity to occipital pole was associated with better performance on landmarks, regardless of modality.

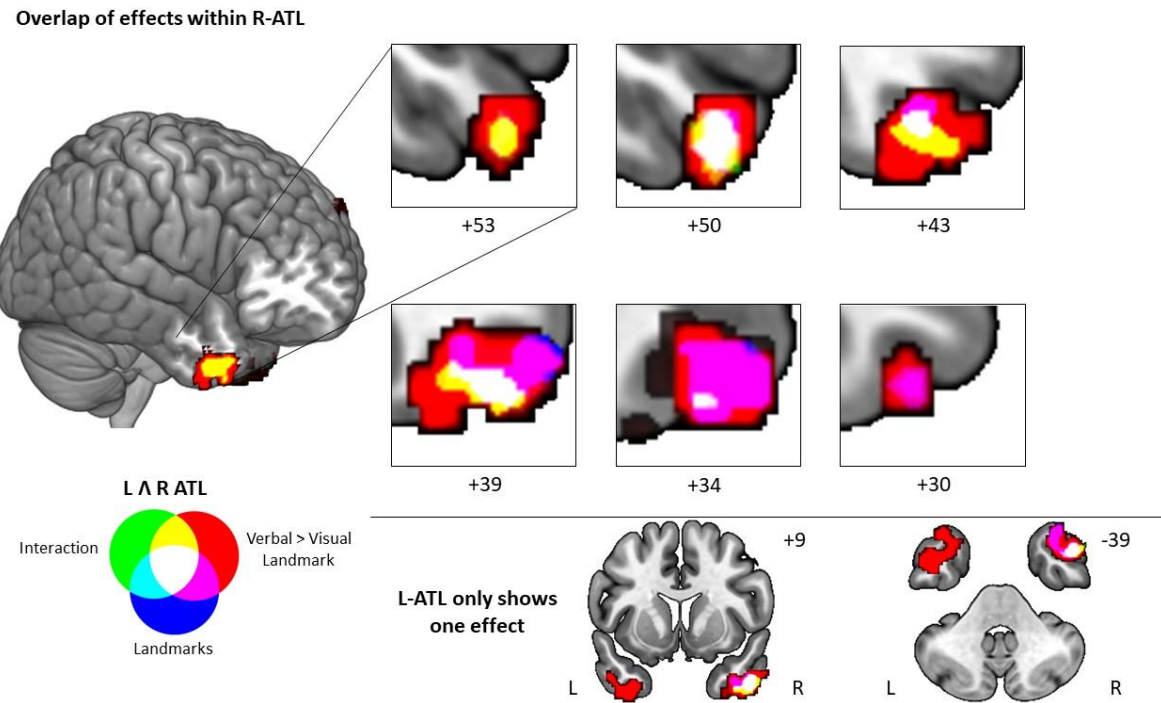


Figure 7. Results of our analysis that fell within left and right ATL (centred on the temporal pole); all of these effects relate to better processing of landmarks, especially in the visual modality. Top panel: Landmarks results that fell in the right temporal lobe and sagittal slices that highlight their topography. Bottom panel: Selected coronal and axial slices that allow comparison between the only effect observed in left ATL with the ones observed in right ATL.

4. Discussion

This study examined the relationship between individual differences in the intrinsic connectivity of left and right ATL and performance on semantic tasks that involved (i) different modalities of presentation (pictures vs. words) and (ii) knowledge of specific people versus landmarks. Previous work has suggested that while the functions of left and right ATL are more similar than they are different, there is some subtle hemispheric specialisation according to modality – in particular, patients with more damage to right ATL can show greater impairment on picture-based tasks (particularly faces), while patients with greater left ATL damage can have particular difficulty accessing knowledge from people's names (Gainotti, 2007; Gainotti and Marra, 2011; Snowden et al., 2004). Moreover, even though bilateral ATL is implicated in knowledge of unique entities across categories (both famous people and landmarks), hemispheric differences relating to semantic category could still

emerge, according to the “graded hub” account (Rice et al., 2015a), if left and right ATL show a degree of difference in their connectivity to posterior visual regions that are differentially implicated in conceptual representation for people and places. This is because concepts are thought to emerge from the interaction of the heteromodal ATL hub with “embodied” unimodal “spoke” systems that provide concrete features, which may be crucial for the differentiation of highly-related concepts (Clarke et al., 2013, 2010; Mollo et al., 2017), such as different famous people or buildings.

We used two ATL seeds derived from functionally-defined peaks for left and right ATL, and identified two key behavioural associations with intrinsic connectivity. (i) We found that stronger connectivity from right ATL relative to left to a region in medial / polar occipital cortex was associated with more efficient retrieval of semantic information about famous landmarks (such as determining whether the Eiffel Tower is European), regardless of the modality of presentation. (ii) We also found that when left and right ATL showed strong connectivity to each other (i.e., the system was strongly bilateral), participants were more efficient at retrieving information about landmarks when these items were presented as pictures instead of words. Our exploratory study did not find associations between hemispheric differences in ATL connectivity and the behavioural contrast of faces and names, even though this is the pattern highlighted strongly in the neuropsychological literature.

The first of our findings -- that efficient categorisation of landmarks is linked to stronger intrinsic connectivity between right ATL and medial regions near the occipital pole -- is consistent with a key role for vision in supporting this category. This cluster fell within the occipital pole, overlapping with primary visual regions. Studies have shown that while bilateral ATL is implicated in knowledge of unique entities across categories (e.g. people and landmarks), posterior visual regions show clear dissociations between these types of concepts (Fairhall et al., 2014; Fairhall and Caramazza, 2013; Wang et al., 2016). Within the visual system, this category distinction has most commonly been studied using pictures as stimuli: the perception of landmarks and scenes activates sites within lingual gyrus, adjacent to our connectivity-derived cluster, as well as medial and ventral regions in parahippocampal place area and retrosplenial cortex (Aguirre and D’Esposito, 1999; Spiers and Maguire, 2007, 2004; Ungerleider, 1982; Yoder et al., 2011); in contrast, face perception more strongly

recruits the occipital and fusiform face areas (Grill-Spector, 2003) along with posterior superior temporal sulcus (Kanwisher et al., 1997; Gauthier et al., 2000; for a review, see Grill-Spector, 2003). However, it has also been shown that this differential visual response by semantic category extends beyond picture tasks, such that category-selective visual regions also show a heteromodal response (Fairhall et al., 2014).

Previous research motivated by the hub-and-spokes account of conceptual knowledge (Lambon Ralph et al., 2017; Patterson et al., 2007) has shown that the dynamic interaction of ventral ATL with medial occipital cortex is essential to the representation and retrieval of visual concepts, even when these are accessed via words (Chiou et al., 2018; Chiou and Lambon Ralph, 2019). In this way, our knowledge of the world draws on “embodied” sensory codes, as well as on heteromodal and more abstract conceptual representations in ATL (Barsalou, 1999; Barsalou et al., 2003; Meteyard et al., 2012; Reilly et al., 2016). In human navigation, landmarks are predominantly visual (although some landmarks, such as a waterfall, may be supplemented by sound). The finding that stronger intrinsic connectivity between right ATL and medial visual cortex is associated with more efficient semantic retrieval for landmarks, regardless of modality, adds to this body of evidence. Right ATL has stronger intrinsic connectivity with medial visual cortex than left ATL (Gonzalez Alam et al., 2019), and participants who show this pattern more strongly show better semantic retrieval for landmarks, perhaps because this category requires strong visuo-spatial imagery.

The second of our findings suggests that there are some functional benefits resulting from strong intrinsic connectivity between the two ATLs. This pattern might be expected for a bilateral semantic representation system: patients with bilateral ATL atrophy who have semantic dementia show more substantial semantic deficits than patients with unilateral ATL lesions following resection for temporal lobe epilepsy (Lambon Ralph et al., 2012; Rice et al., 2018a), perhaps because the two ATLs show a high degree of connectivity (Gonzalez Alam et al., 2019) and consequently the semantic store is only partially divided between left and right hemispheres. This neuropsychological data is accommodated by a model of ATL with strong bilateral connections, as well as somewhat distinct connections from left and right ATL to other brain regions (Schapiro et al., 2013). However, this benefit of bilateral connections between the two ATLs was shown in the current study to be unequal across tasks. Strong cross-hemispheric connectivity particularly benefits tasks which probe knowledge of places and that also use pictorial inputs – perhaps because, in these circumstances, right-lateralised visual-spatial representations (Liu et al., 2009; Stevens et al.,

2012) need to be integrated with a left-lateralised semantic retrieval network (including IFG and posterior temporal regions), shown to activate more strongly to semantic decisions about landmarks than people in an on-line fMRI study employing the same tasks (Rice et al., 2018b). The fact that the landmark pictures were presented together with naturalistic backgrounds, while the faces were presented on relatively plain backgrounds, might also have contributed to this effect, by increasing reliance of the landmark condition on spatial information and subtle visual cues in the environment. One as yet untested hypothesis emerging from this finding is that patients with semantic dementia might have more severe difficulties in retrieving conceptual information from visual landmark pictures (compared with the categorisation of famous faces and names, and the names of landmarks), reflecting their highly bilateral atrophy.

In conclusion, this study shows that individual differences in the intrinsic connectivity of left and right ATL are associated with effects of category and modality on semantic efficiency in the processing of landmarks. These effects can be interpreted in terms of graded differences in the strengths of inputs from ‘spoke’ regions, such as regions of visual cortex, to a bilateral yet partially segregated semantic ‘hub’, encompassing left and right ATL.

Acknowledgements

We would like to thank the students that helped with data collection: Melinda Bjolseth, Sophie Colgan, Lucy Milne, Clara Scatola, Nikita Schaap, George Shone, Molly Sibson-Flood, Dragos Teodorov and Molly Wilson.

Supplementary Materials

1. Single seed results

We carried out behavioural regressions on the intrinsic connectivity of left ATL and right ATL separately. The results of these single seed analyses fall within the effects described in the main text for the combined (left plus right ATL) and differential (left versus right ATL) analyses. Left ATL showed two significant results, presented in Figure S1: participants with stronger connectivity from this left ATL seed to a right ATL cluster showed a better performance for visual relative to verbal landmarks; we also found a category by modality interaction in the same region.

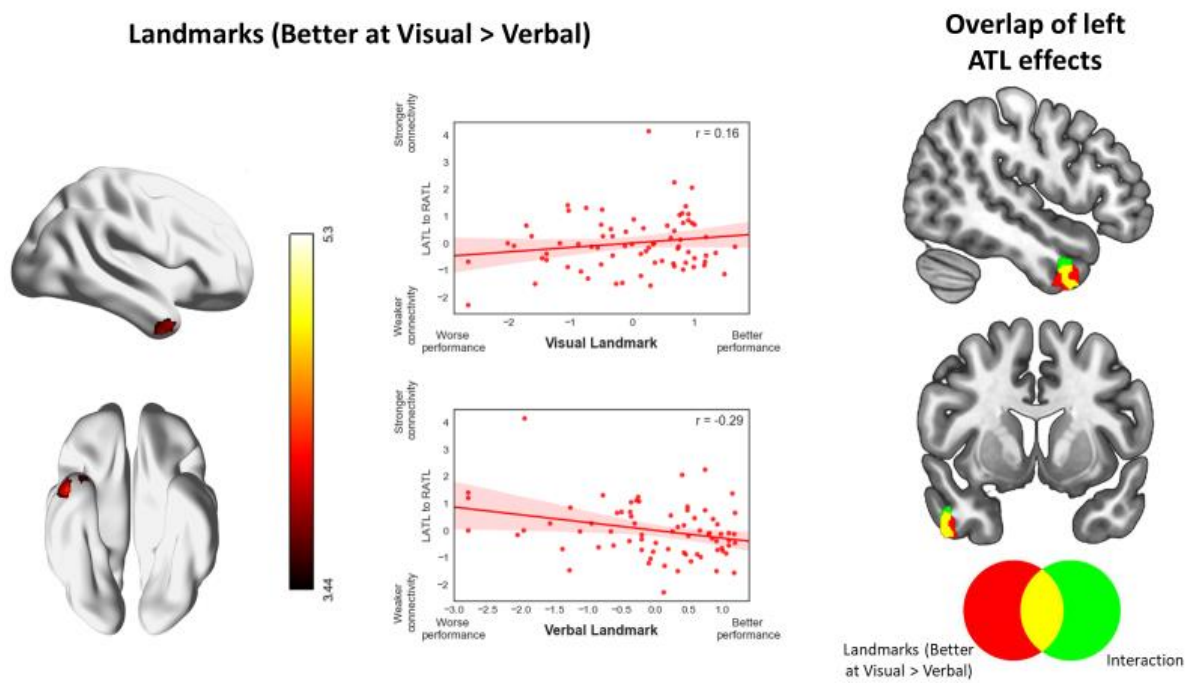


Figure S1. The connectivity between a right temporal pole cluster and the left ATL seed was associated with better performance at visual relative to verbal landmark judgements ($Z=3.1$, $p=.05$, Bonferroni-corrected for 4 models). The scatterplots depict the mean-centred efficiency scores (given in z-scores), plotted as a function of the normalised functional connectivity (i.e. scaled to the global mean) between the right temporal pole cluster depicted in the figure and the left ATL seed. This cluster overlapped with an interaction effect, as depicted in the right column of the figure.

Right ATL also showed two significant results: participants with stronger connectivity from the right ATL seed to a more anterior bilateral temporal pole cluster were better at visual

relative to verbal landmark judgements, as well as generally better at visual landmarks. These results are shown in Figure S2.

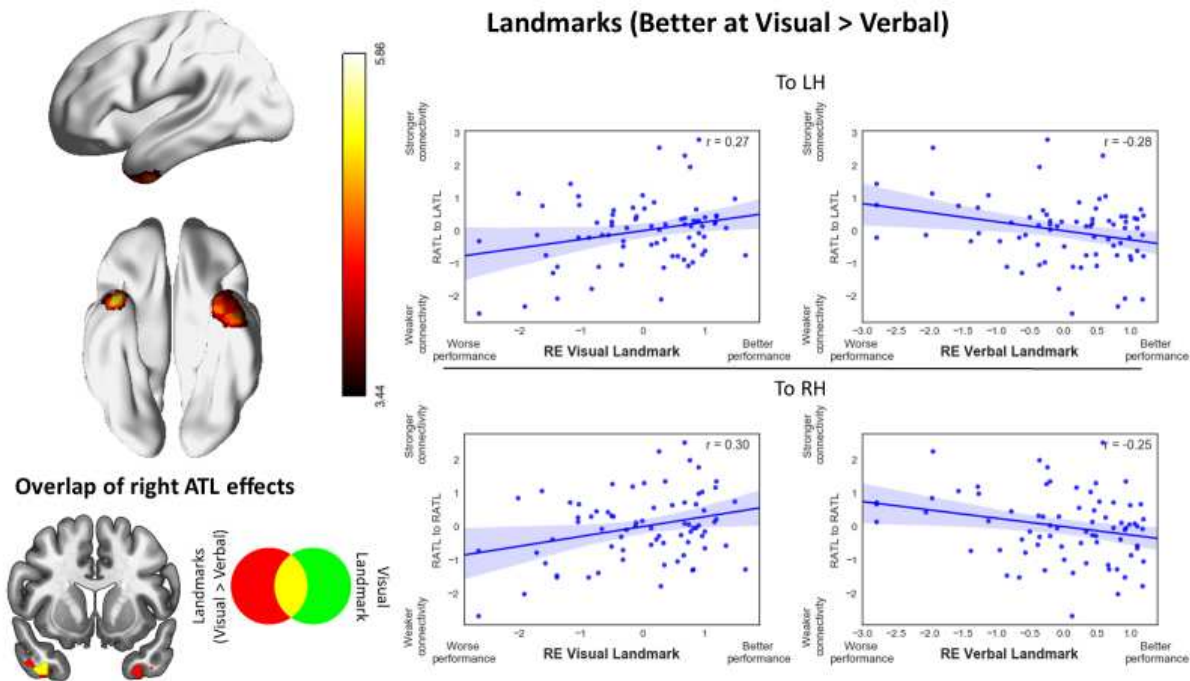


Figure S2. The connectivity between bilateral ATL clusters and the right ATL seed was associated with better performance at visual relative to verbal landmark judgements ($Z=3.1$, $p=.05$, Bonferroni-corrected for 4 models). The scatterplots depict the mean-centred efficiency scores (given in z-scores), plotted as a function of the normalised functional connectivity (i.e. scaled to the global mean) between the left and right ATL clusters depicted in the figure and the left and right ATL seeds. The bottom left section of the figure shows that the right ATL cluster for the visual > verbal landmark contrast (shown in red) overlapped with the main effect of being good at the visual landmark condition (shown in green).

2. Control analysis with a sign-flipped homotopic seed

We compared the results for functionally-defined seeds (see main text) with homotopic sites in left and right ATL, which had equivalent MNI coordinates across the two hemispheres. The homotopic right ATL seed was created by flipping the functionally-defined left ATL seed into the right hemisphere (changing the sign of the x coordinate in MNI space from negative to positive). This analysis allowed us to establish if the same behavioural associations could be observed using homotopic seeds, therefore confirming that the results in the main text do not arise from the subtly different locations of left and right ATL seeds.

This is important given that the functional connectivity of ATL changes gradually across this region (Jackson et al., 2017, 2016; Rice et al., 2015a).

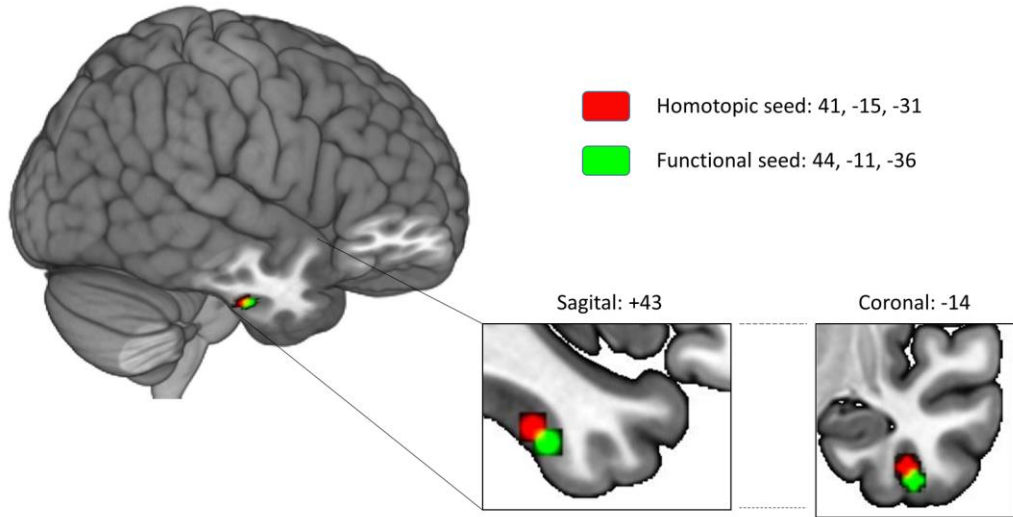


Figure S3. Depiction of the position of the homotopic and functional seeds in right ATL, and their spatial relation to each other.

We examined the mean intrinsic connectivity of left ATL (see main text) and its right homotopic. We examined the single seed mean connectivity for each ATL, as well as mean connectivity from both seeds combined, and differential left vs. right connectivity. The results are shown in Figure S4. The RH homotopic seed showed a similar pattern to the LH functional seed: it showed temporal lobe connectivity, albeit less continuous in the LH and more restricted to the ventral temporal lobes, with a separate cluster for angular gyrus that extended more posteriorly than for the left ATL. Unlike left ATL, the RH homotopic did not show connectivity to the central sulcus, but there was high intrinsic connectivity with superior frontal gyrus and medial orbitofrontal cortex extending posteriorly to the posterior cingulate cortex; this RH site also showed weak intrinsic connectivity with medial occipital, paracingulate and right insular/orbitofrontal regions (Figure S4, second row). This pattern is similar to that described by Gonzalez Alam et al. (2019). An analysis giving equal weight to both left and right ATL seeds captured this similarity between the maps (Figure S4, third row). Significant differences between the left and right ATL were only observed in the ventral regions centred around our seeds (Figure S4, fourth row). Lastly, a direct comparison

between the homotopic and functional right ATL seeds revealed stronger connectivity for the homotopic seed in bilateral LOC, lingual gyrus, posterior cingulate cortex and medial temporal cortex, and stronger connectivity with the functional seed in bilateral vATL, right frontal pole and left temporo-parietal junction (Figure S4, bottom row).

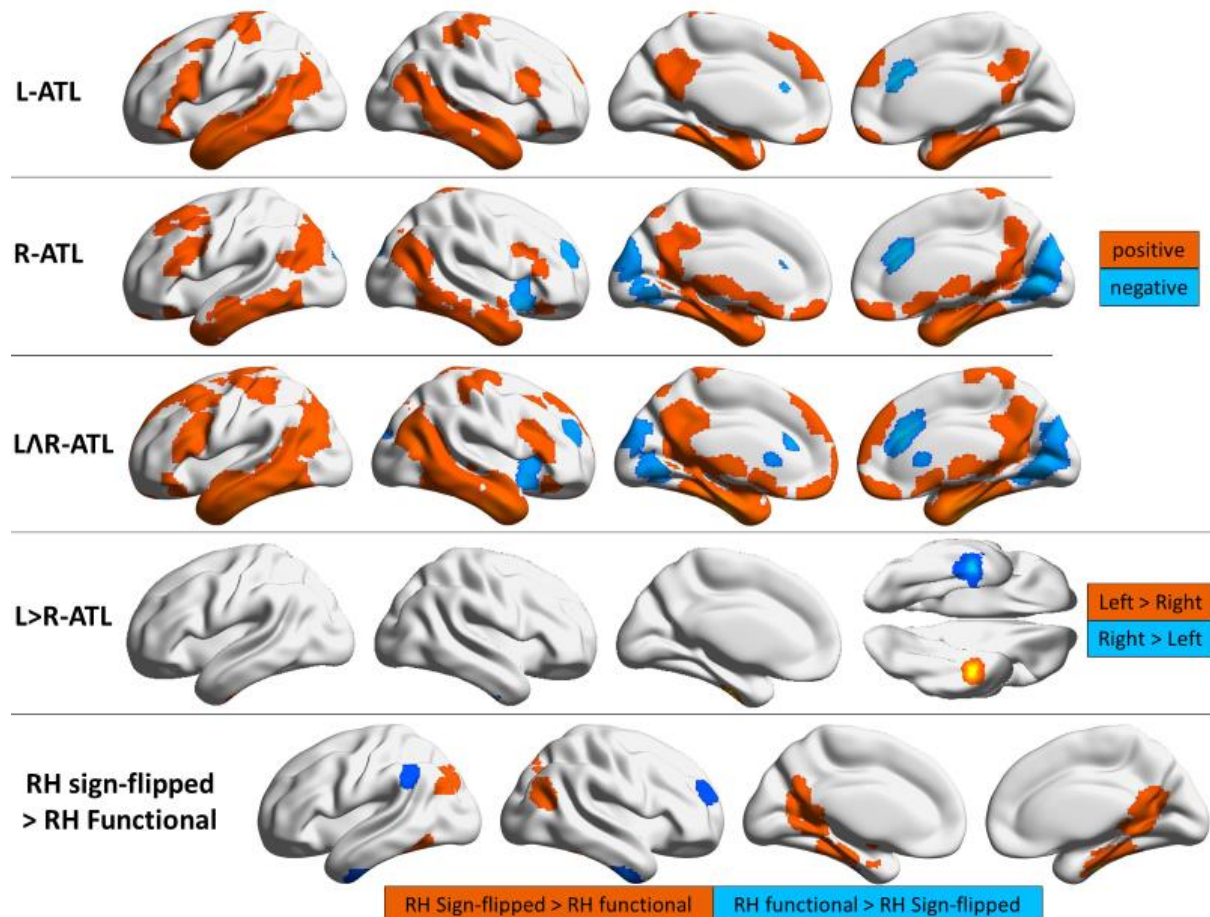


Figure S4. Resting state connectivity for the homotopic peak in right ATL, its common and differential connectivity with functionally-defined left ATL (from Rice et al., 2018), and a comparison of the functionally-defined right ATL with the right hemisphere seed determined through sign-flipping. For the single seeds and mean, the warm and cool colours represent the positive and negative patterns of connectivity respectively, while for the difference analysis, the warm and cool colours represent left and right connectivity respectively. In the last row, stronger connectivity for the homotopic seed is represented by warm colours while stronger connectivity for the functional seed is depicted in cool colours. The group maps are thresholded at $z = 3.1$, $p = 0.05$.

References

Aguirre, G.K., D'Esposito, M., 1999. Topographical disorientation: a synthesis and taxonomy. *Brain* 122, 1613–1628. <https://doi.org/10.1093/brain/122.9.1613>

Bajada, C.J., Trujillo-Barreto, N.J., Parker, G.J.M.M., Cloutman, L.L., Lambon Ralph, M.A., 2019. A structural connectivity convergence zone in the ventral and anterior temporal lobes: Data-driven evidence from structural imaging. *Cortex* 120, 298–307. <https://doi.org/https://doi.org/10.1016/j.cortex.2019.06.014>

Barsalou, L.W., 1999. Perceptual symbol systems. *Behav. Brain Sci.* 22, 577–609; discussion 610–660.

Barsalou, L.W., Simmons, W.K., Barbey, A.K., Wilson, C.D., 2003. Grounding conceptual knowledge in modality-specific systems. *Trends Cogn. Sci.* 7, 84–91. [https://doi.org/https://doi.org/10.1016/S1364-6613\(02\)00029-3](https://doi.org/https://doi.org/10.1016/S1364-6613(02)00029-3)

Behzadi, Y., Restom, K., Liau, J., Liu, T.T., 2007. A component based noise correction method (CompCor) for BOLD and perfusion based fMRI. *Neuroimage* 37, 90–101. <https://doi.org/10.1016/j.neuroimage.2007.04.042>

Binney, R.J., Embleton, K. V., Jefferies, E., Parker, G.J.M., Lambon Ralph, M. a., 2010. The Ventral and Inferolateral Aspects of the Anterior Temporal Lobe Are Crucial in Semantic Memory: Evidence from a Novel Direct Comparison of Distortion-Corrected fMRI, rTMS, and Semantic Dementia. *Cereb. Cortex* 20, 2728–2738. <https://doi.org/10.1093/cercor/bhq019>

Binney, R.J., Lambon Ralph, M.A., 2015. Using a combination of fMRI and anterior temporal lobe rTMS to measure intrinsic and induced activation changes across the semantic cognition network. *Neuropsychologia* 76, 170–181. <https://doi.org/10.1016/j.neuropsychologia.2014.11.009>

Binney, R.J., Parker, G.J.M., Lambon Ralph, M.A., 2012. Convergent Connectivity and Graded Specialization in the Rostral Human Temporal Lobe as Revealed by Diffusion-Weighted Imaging Probabilistic Tractography. *J. Cogn. Neurosci.* 24, 1998–2014. https://doi.org/10.1162/jocn_a_00263

Bright, P., Moss, H., Tyler, L.K., 2004. Unitary vs multiple semantics: PET studies of word and picture processing. *Brain Lang.* 89, 417–432.

<https://doi.org/10.1016/j.bandl.2004.01.010>

Butler, C.R., Brambati, S.M., Miller, B.L., Gorno-Tempini, M.-L., 2009. The neural correlates of verbal and nonverbal semantic processing deficits in neurodegenerative disease. *Cogn. Behav. Neurol.* 22, 73–80.

<https://doi.org/10.1097/WNN.0b013e318197925d>

Chai, X.J., Castanon, A.N., Ongur, D., Whitfield-Gabrieli, S., 2012. Anticorrelations in resting state networks without global signal regression. *Neuroimage* 59, 1420–1428. <https://doi.org/10.1016/j.neuroimage.2011.08.048>

Chiou, R., Humphreys, G.F., Jung, J.Y., Lambon Ralph, M.A., 2018. Controlled semantic cognition relies upon dynamic and flexible interactions between the executive ‘semantic control’ and hub-and-spoke ‘semantic representation’ systems. *Cortex* 103, 100–116. <https://doi.org/10.1016/j.cortex.2018.02.018>

Chiou, R., Lambon Ralph, M.A., 2019. Unveiling the dynamic interplay between the hub-and spoke-components of the brain’s semantic system and its impact on human behaviour, *NeuroImage*. Elsevier Inc. <https://doi.org/10.1016/j.neuroimage.2019.05.059>

Clarke, A., Taylor, K.I., Devereux, B., Randall, B., Tyler, L.K., 2013. From Perception to Conception: How Meaningful Objects Are Processed over Time. *Cereb. Cortex* 23, 187–197. <https://doi.org/10.1093/cercor/bhs002>

Clarke, A., Taylor, K.I., Tyler, L.K., 2010. The Evolution of Meaning: Spatio-temporal Dynamics of Visual Object Recognition. *J. Cogn. Neurosci.* 23, 1887–1899. <https://doi.org/10.1162/jocn.2010.21544>

Cole, M.W., Bassett, D.S., Power, J.D., Braver, T.S., Petersen, S.E., 2014. Intrinsic and task-evoked network architectures of the human brain. *Neuron* 83, 238–251. <https://doi.org/10.1016/j.neuron.2014.05.014>

Damasio, H., Tranel, D., Grabowski, T., Adolphs, R., Damasio, A., 2004. Neural systems behind word and concept retrieval. *Cognition* 92, 179–229. <https://doi.org/10.1016/j.cognition.2002.07.001>

Ding, J., Chen, K., Liu, H., Huang, L., Chen, Y., Lv, Y., Yang, Q., Guo, Q., Han, Z., Lambon Ralph, M.A., 2020. A unified neurocognitive model of semantics language social behaviour and face recognition in semantic dementia. *Nat. Commun.* 11, 1–14.

<https://doi.org/10.1038/s41467-020-16089-9>

Draheim, C., Hicks, K.L., Engle, R.W., 2016. Combining Reaction Time and Accuracy: The Relationship Between Working Memory Capacity and Task Switching as a Case Example. *Perspect. Psychol. Sci.* 11, 133–155.

<https://doi.org/10.1177/1745691615596990>

Eklund, A., Nichols, T.E., Knutsson, H., 2016. Cluster failure: Why fMRI inferences for spatial extent have inflated false-positive rates. *Proc. Natl. Acad. Sci.* 113, 201602413.

<https://doi.org/10.1073/pnas.1602413113>

Evans, M., Krieger-Redwood, K., Gonzalez Alam, T.R.J., Smallwood, J., Jefferies, E., 2020. Controlled semantic summation correlates with intrinsic connectivity between default mode and control networks. *Cortex* 129, 356–375.

<https://doi.org/https://doi.org/10.1016/j.cortex.2020.04.032>

Fairhall, S.L., Anzellotti, S., Ubaldi, S., Caramazza, A., 2014. Person- and place-selective neural substrates for entity-specific semantic access. *Cereb. Cortex* 24, 1687–1696.

<https://doi.org/10.1093/cercor/bht039>

Fairhall, S.L., Caramazza, A., 2013. Category-selective neural substrates for person- and place-related concepts. *Cortex* 49, 2748–2757.

<https://doi.org/10.1016/j.cortex.2013.05.010>

Fernandino, L., Binder, J.R., Desai, R.H., Pendl, S.L., Humphries, C.J., Gross, W.L., Conant, L.L., Seidenberg, M.S., 2016. Concept Representation Reflects Multimodal Abstraction: A Framework for Embodied Semantics. *Cereb. Cortex* 26, 2018–2034.

<https://doi.org/10.1093/cercor/bhv020>

Gainotti, G., 2013. Is the right anterior temporal variant of prosopagnosia a form of “associative prosopagnosia” or a form of “multimodal person recognition disorder”? *Neuropsychol. Rev.* 23, 99–110. <https://doi.org/10.1007/s11065-013-9232-7>

Gainotti, G., 2012. The format of conceptual representations disrupted in semantic dementia: A position paper. *Cortex* 48, 521–529. <https://doi.org/10.1016/j.cortex.2011.06.019>

Gainotti, G., 2007. Different patterns of famous people recognition disorders in patients with right and left anterior temporal lesions: A systematic review. *Neuropsychologia* 45, 1591–1607. <https://doi.org/10.1016/j.neuropsychologia.2006.12.013>

Gainotti, G., Marra, C., 2011. Differential contribution of right and left temporo-occipital and anterior temporal lesions to face recognition disorders. *Front. Hum. Neurosci.* 5, 1–11. <https://doi.org/10.3389/fnhum.2011.00055>

Gauthier, I., Tarr, M.J., Moylan, J., Skudlarski, P., Gore, J.C., Anderson, A.W., 2000. The Fusiform “Face Area” is Part of a Network that Processes Faces at the Individual Level. *J. Cogn. Neurosci.* 12, 495–504. <https://doi.org/10.1162/089892900562165>

Gonzalez Alam, T., Murphy, C., Smallwood, J., Jefferies, E., 2018. Meaningful inhibition: Exploring the role of meaning and modality in response inhibition. *Neuroimage* 181, 108–119. <https://doi.org/10.1016/j.neuroimage.2018.06.074>

Gonzalez Alam, T.R. del J., Karapanagiotidis, T., Smallwood, J., Jefferies, E., 2019. Degrees of lateralisation in semantic cognition: Evidence from intrinsic connectivity. *Neuroimage* 202, 116089. <https://doi.org/10.1016/j.neuroimage.2019.116089>

Gorgolewski, K.J., Varoquaux, G., Rivera, G., Schwarz, Y., Ghosh, S.S., Maumet, C., Sochat, V. V., Nichols, T.E., Poldrack, R.A., Poline, J.-B., Yarkoni, T., Margulies, D.S., 2015. NeuroVault.org: a web-based repository for collecting and sharing unthresholded statistical maps of the human brain. *Front. Neuroinform.* 9, 1–9. <https://doi.org/10.3389/fninf.2015.00008>

Gorno-Tempini, M.L., Price, C.J., 2001. Identification of famous faces and buildings. A functional neuroimaging study of semantically unique items. *Brain* 124, 2087–2097. <https://doi.org/10.1093/brain/124.10.2087>

Gorno-Tempini, M.L., Price, C.J., Josephs, O., Vandenberghe, R., Cappa, S.F., Kapur, N., Frackowiak, R.S., 1998. The neural systems sustaining face and proper-name processing. *Brain* 121 (Pt 11), 2103–2118. <https://doi.org/10.1093/brain/121.11.2103>

Grabowski, T.J., Damasio, H., Tranel, D., Boles Ponto, L.L., Hichwa, R.D., Damasio, A.R., 2001. A role for left temporal pole in the retrieval of words for unique entities. *Hum. Brain Mapp.* 13, 199–212.

Grill-Spector, K., 2003. The neural basis of object perception. *Curr. Opin. Neurobiol.* 13, 159–166. [https://doi.org/10.1016/S0959-4388\(03\)00040-0](https://doi.org/10.1016/S0959-4388(03)00040-0)

Ishibashi, R., Pobric, G., Saito, S., Lambon Ralph, M.A., 2016. The neural network for tool-related cognition: An activation likelihood estimation meta-analysis of 70 neuroimaging

contrasts. *Cogn. Neuropsychol.* 33, 241–256.
<https://doi.org/10.1080/02643294.2016.1188798>

Jackson, R.L., Bajada, C.J., Rice, G.E., Cloutman, L.L., Lambon Ralph, M.A., 2017. An emergent functional parcellation of the temporal cortex. *Neuroimage* 1–15.
<https://doi.org/10.1016/j.neuroimage.2017.04.024>

Jackson, R.L., Hoffman, P., Pobric, G., Lambon Ralph, M.A., 2016. The Semantic Network at Work and Rest: Differential Connectivity of Anterior Temporal Lobe Subregions. *J. Neurosci.* 36, 1490–501. <https://doi.org/10.1523/JNEUROSCI.2999-15.2016>

Jackson, R.L., Lambon Ralph, M.A., Pobric, G., 2015. The Timing of Anterior Temporal Lobe Involvement in Semantic Processing. *J. Cogn. Neurosci.* 27, 1388–1396.
<https://doi.org/10.1162/jocn>

Jung, J.Y., Lambon Ralph, M.A., 2016. Mapping the Dynamic Network Interactions Underpinning Cognition: A cTBS-fMRI Study of the Flexible Adaptive Neural System for Semantics. *Cereb. Cortex* 26, 3580–3590. <https://doi.org/10.1093/cercor/bhw149>

Kanwisher, N., McDermott, J., Chun, M.M., 1997. The fusiform face area: a module in human extrastriate cortex specialized for face perception. *J. Neurosci.* 17, 4302–11.
<https://doi.org/10.1098/Rstb.2006.1934>

Lambon Ralph, M.A., Ehsan, S., Baker, G.A., Rogers, T.T., 2012. Semantic memory is impaired in patients with unilateral anterior temporal lobe resection for temporal lobe epilepsy. *Brain* 135, 242–258. <https://doi.org/10.1093/brain/awr325>

Lambon Ralph, M.A., Jefferies, E., Patterson, K., Rogers, T.T., 2017. The neural and computational bases of semantic cognition. *Nat. Rev. Neurosci.* 18, 42–55.
<https://doi.org/10.1038/nrn.2016.150>

Lambon Ralph, M.A., McClelland, J.L., Patterson, K., Galton, C.J., Hodges, J.R., 2001. No right to speak? The relationship between object naming and semantic impairment: neuropsychological evidence and a computational model. *J. Cogn. Neurosci.* 13, 341–356. <https://doi.org/10.1162/08989290151137395>

Liljeström, M., Tarkiainen, A., Parviainen, T., Kujala, J., Numminen, J., Hiltunen, J., Laine, M., Salmelin, R., 2008. Perceiving and naming actions and objects. *Neuroimage* 41, 1132–1141. <https://doi.org/10.1016/j.neuroimage.2008.03.016>

Liu, H., Stufflebeam, S.M., Sepulcre, J., Hedden, T., Buckner, R.L., 2009. Evidence from intrinsic activity that asymmetry of the human brain is controlled by multiple factors. *Proc. Natl. Acad. Sci. U. S. A.* 106, 20499–20503.
<https://doi.org/10.1073/pnas.0908073106>

Luzzi, S., Baldinelli, S., Ranaldi, V., Fabi, K., Cafazzo, V., Fringuelli, F., Silvestrini, M., Provinciali, L., Reverberi, C., Gainotti, G., 2017. Famous faces and voices: Differential profiles in early right and left semantic dementia and in Alzheimer's disease. *Neuropsychologia* 94, 118–128. <https://doi.org/10.1016/j.neuropsychologia.2016.11.020>

Meteyard, L., Cuadrado, S.R., Bahrami, B., Vigliocco, G., 2012. Coming of age: A review of embodiment and the neuroscience of semantics. *Cortex* 48, 788–804.
<https://doi.org/10.1016/j.cortex.2010.11.002>

Mion, M., Patterson, K., Acosta-Cabronero, J., Pengas, G., Izquierdo-Garcia, D., Hong, Y.T., Fryer, T.D., Williams, G.B., Hodges, J.R., Nestor, P.J., 2010. What the left and right anterior fusiform gyri tell us about semantic memory. *Brain* 133, 3256–3268.
<https://doi.org/10.1093/brain/awq272>

Mollo, G., Cornelissen, P.L., Millman, R.E., Ellis, A.W., Jefferies, E., 2017. Oscillatory dynamics supporting semantic cognition: Meg evidence for the contribution of the anterior temporal lobe hub and modality-specific spokes. *PLoS One* 12, 1–25.
<https://doi.org/10.1371/journal.pone.0169269>

Mollo, G., Jefferies, E., Cornelissen, P., Gennari, S.P., 2018. Context-dependent lexical ambiguity resolution: MEG evidence for the time-course of activity in left inferior frontal gyrus and posterior middle temporal gyrus. *Brain Lang.* 177–178, 23–36.
<https://doi.org/10.1016/j.bandl.2018.01.001>

Mollo, G., Karapanagiotidis, T., Bernhardt, B.C., Murphy, C.E., Smallwood, J., Jefferies, E., 2016. An individual differences analysis of the neurocognitive architecture of the semantic system at rest. *Brain Cogn.* 109, 112–123.
<https://doi.org/10.1016/j.bandc.2016.07.003>

Moss, H.E., Rodd, J.M., Stamatakis, E.A., Bright, P., Tyler, L.K., 2005. Anteromedial temporal cortex supports fine-grained differentiation among objects. *Cereb. Cortex* 15, 616–627. <https://doi.org/10.1093/cercor/bhh163>

Moss, H.E., Tyler, L.K., Durrant-Peatfield, M., Bunn, E.M., 1998. "Two eyes of a see-through": Impaired and intact semantic knowledge in a case of selective deficit for living things." *Neurocase*. <https://doi.org/10.1093/neucas/4.4.291>

Murphy, C., Rueschemeyer, S.A., Watson, D., Karapanagiotidis, T., Smallwood, J., Jefferies, E., 2017. Fractionating the anterior temporal lobe: MVPA reveals differential responses to input and conceptual modality. *Neuroimage* 147, 19–31.
<https://doi.org/10.1016/j.neuroimage.2016.11.067>

Murphy, K., Birn, R.M., Handwerker, D.A., Jones, T.B., Bandettini, P.A., 2009. The impact of global signal regression on resting state correlations: Are anti-correlated networks introduced? *Neuroimage* 44, 893–905. <https://doi.org/10.1016/j.neuroimage.2008.09.036>

Olson, I.R., McCoy, D., Klobusicky, E., Ross, L.A., 2013. Social cognition and the anterior temporal lobes: A review and theoretical framework. *Soc. Cogn. Affect. Neurosci.* 8, 123–133. <https://doi.org/10.1093/scan/nss119>

Olson, I.R., Plotzker, A., Ezzyat, Y., 2007. The Enigmatic temporal pole: A review of findings on social and emotional processing. *Brain* 130, 1718–1731.
<https://doi.org/10.1093/brain/awm052>

Papinutto, N., Galantucci, S., Luisa Mandelli, M., Gesierich, B., Jovicich, J., Caverzasi, E., Henry, R.G., Seeley, W.W., Miller, B.L., Shapiro, K.A., Luisa Gorno-Tempini, M., 2016. Structural connectivity of the human anterior temporal lobe: A diffusion magnetic resonance imaging study. *Hum. Brain Mapp.* 00, n/a-n/a.
<https://doi.org/10.1002/hbm.23167>

Patterson, K., Nestor, P.J., Rogers, T.T., 2007. Where do you know what you know? The representation of semantic knowledge in the human brain. *Nat. Rev. Neurosci.* 8, 976–987. <https://doi.org/10.1038/nrn2277>

Pobric, G., Jefferies, E., Lambon Ralph, M.A., 2010. Amodal semantic representations depend on both anterior temporal lobes: Evidence from repetitive transcranial magnetic stimulation. *Neuropsychologia* 48, 1336–1342.
<https://doi.org/10.1016/j.neuropsychologia.2009.12.036>

Pobric, G., Jefferies, E., Lambon Ralph, M.A., 2007. Anterior temporal lobes mediate semantic representation: mimicking semantic dementia by using rTMS in normal

participants. *Proc. Natl. Acad. Sci. U. S. A.* 104, 20137–20141. <https://doi.org/10.1073/pnas.0707383104>

Poerio, G.L., Sormaz, M., Wang, H.T., Margulies, D., Jefferies, E., Smallwood, J., 2017. The role of the default mode network in component processes underlying the wandering mind. *Soc. Cogn. Affect. Neurosci.* 12, 1047–1062. <https://doi.org/10.1093/scan/nsx041>

Reilly, J., Peelle, J.E., Garcia, A., Crutch, S.J., 2016. Linking somatic and symbolic representation in semantic memory: the dynamic multilevel reactivation framework. *Psychon. Bull. Rev.* 23, 1002–1014. <https://doi.org/10.3758/s13423-015-0824-5>

Rice, G.E., Caswell, H., Moore, P., Ralph, M.A.L., Hoffman, P., 2018a. Revealing the Dynamic Modulations That Underpin a Resilient Neural Network for Semantic Cognition: An fMRI Investigation in Patients With Anterior Temporal Lobe Resection. *Cereb. Cortex* 28, 3004–3016. <https://doi.org/10.1093/cercor/bhy116>

Rice, G.E., Hoffman, P., Binney, R.J., Lambon Ralph, M.A., 2018b. Concrete versus abstract forms of social concept: an fMRI comparison of knowledge about people versus social terms. *Philos. Trans. R. Soc. B Biol. Sci.* 373, 20170136. <https://doi.org/10.1098/rstb.2017.0136>

Rice, G.E., Hoffman, P., Lambon Ralph, M.A., 2015a. Graded specialization within and between the anterior temporal lobes. *Ann. N. Y. Acad. Sci.* 1359, 84–97. <https://doi.org/10.1111/nyas.12951>

Rice, G.E., Lambon Ralph, M.A., Hoffman, P., 2015b. The Roles of Left Versus Right Anterior Temporal Lobes in Conceptual Knowledge: An ALE Meta-analysis of 97 Functional Neuroimaging Studies. *Cereb. Cortex* 25, 4374–4391. <https://doi.org/10.1093/cercor/bhv024>

Rogers, T.T., Hocking, J., Mechelli, A., Patterson, K., Price, C., 2005. Fusiform Activation to Animals is Driven by the Process, Not the Stimulus. *J. Cogn. Neurosci.* 17, 434–445. <https://doi.org/10.1162/0898929053279531>

Rogers, T.T., Hocking, J., Noppeney, U., Mechelli, A., Gorno-Tempini, M.L., Patterson, K., Price, C.J., 2006. Anterior temporal cortex and semantic memory: Reconciling findings from neuropsychology and functional imaging. *Cogn. Affect. Behav. Neurosci.* 6, 201–213. <https://doi.org/10.3758/CABN.6.3.201>

Rogers, T.T., Patterson, K., Jefferies, E., Lambon Ralph, M.A., 2015. Disorders of representation and control in semantic cognition: Effects of familiarity, typicality, and specificity. *Neuropsychologia* 76, 220–239.
<https://doi.org/10.1016/j.neuropsychologia.2015.04.015>

Ross, L.A., Olson, I.R., 2012. What's unique about unique entities? An fMRI investigation of the semantics of famous faces and landmarks. *Cereb. Cortex* 22, 2005–2015.
<https://doi.org/10.1093/cercor/bhr274>

Ross, L.A., Olson, I.R., 2010. Social cognition and the anterior temporal lobes. *Neuroimage* 49, 3452–3462. <https://doi.org/10.1016/j.neuroimage.2009.11.012>

Schapiro, A.C., McClelland, J.L., Welbourne, S.R., Rogers, T.T., Lambon Ralph, M.A., 2013. Why Bilateral Damage Is Worse than Unilateral Damage to the Brain. *J. Cogn. Neurosci.* 25, 2107–2123. https://doi.org/10.1162/jocn_a_00441

Smith, S.M., Fox, P.T., Miller, K.L., Glahn, D.C., Fox, P.M., Mackay, C.E., Filippini, N., Watkins, K.E., Toro, R., Laird, A.R., Beckmann, C.F., 2009. Correspondence of the brain's functional architecture during activation and rest. *Proc. Natl. Acad. Sci. U. S. A.* 106, 13040–13045. <https://doi.org/10.1073/pnas.0905267106>

Snowden, J.S., Harris, J.M., Thompson, J.C., Kobylecki, C., Jones, M., Richardson, A.M., Neary, D., 2017. Semantic dementia and the left and right temporal lobes. *Cortex*. <https://doi.org/10.1016/j.cortex.2017.08.024>

Snowden, J.S., Thompson, J.C., Neary, D., 2012. Famous people knowledge and the right and left temporal lobes. *Behav. Neurol.* 25, 35–44. <https://doi.org/10.3233/BEN-2012-0347>

Snowden, J.S., Thompson, J.C., Neary, D., 2004. Knowledge of famous faces and names in semantic dementia. *Brain* 127, 860–872. <https://doi.org/10.1093/brain/awh099>

Sormaz, M., Jefferies, E., Bernhardt, B.C., Karapanagiotidis, T., Mollo, G., Bernasconi, N., Bernasconi, A., Hartley, T., Smallwood, J., 2017. Knowing what from where: Hippocampal connectivity with temporoparietal cortex at rest is linked to individual differences in semantic and topographic memory. *Neuroimage* 152, 400–410.
<https://doi.org/10.1016/j.neuroimage.2017.02.071>

Spiers, H.J., Maguire, E.A., 2007. The neuroscience of remote spatial memory: A tale of two

cities. *Neuroscience* 149, 7–27. <https://doi.org/10.1016/j.neuroscience.2007.06.056>

Spiers, H.J., Maguire, E.A., 2004. A “landmark” study on the neural basis of navigation. *Nat. Neurosci.* 7, 572–574. <https://doi.org/10.1038/nn0604-572>

Stevens, W.D., Kahn, I., Wig, G.S., Schacter, D.L., 2012. Hemispheric asymmetry of visual scene processing in the human brain: Evidence from repetition priming and intrinsic activity. *Cereb. Cortex* 22, 1935–1949. <https://doi.org/10.1093/cercor/bhr273>

Tranel, D., 2006. Impaired naming of unique landmarks is associated with left temporal polar damage. *Neuropsychology* 20, 1–10. <https://doi.org/10.1037/0894-4105.20.1.1>

Tranel, D., Damasio, H., Damasio, A.R., 1997. A neural basis for the retrieval of conceptual knowledge. *Neuropsychologia* 35, 1319–1327. [https://doi.org/10.1016/S0028-3932\(97\)00085-7](https://doi.org/10.1016/S0028-3932(97)00085-7)

Tranel, D., Grabowski, T.J., Lyon, J., Damasio, H., 2005. Naming the Same Entities from Visual or from Auditory Stimulation Engages Similar Regions of Left Inferotemporal Cortices. *J. Cogn. Neurosci.* <https://doi.org/10.1162/0898929055002508>

Ungerleider, L.G., 1982. Two cortical visual systems. *Anal. Vis. Behav.* 549–586.

Van Dijk, K.R.A., Hedden, T., Venkataraman, A., Evans, K.C., Lazar, S.W., Buckner, R.L., 2010. Intrinsic functional connectivity as a tool for human connectomics: Theory, properties, and optimization. *J. Neurophysiol.* 103, 297–321. <https://doi.org/10.1152/jn.00783.2009>

Vandenberghe, R., Price, C., Wise, R., Josephs, O., Frackowiak, R.S.J., 1996. Functional anatomy of a common semantic system for words and pictures. *Nature* 383, 254–256. <https://doi.org/10.1038/383254a0>

Vandierendonck, A., 2017. A comparison of methods to combine speed and accuracy measures of performance: A rejoinder on the binning procedure. *Behav. Res. Methods* 49, 653–673. <https://doi.org/10.3758/s13428-016-0721-5>

Vatansever, D., Bzdok, D., Wang, H., Mollo, G., Sormaz, M., Murphy, C., Karapanagiotidis, T., Smallwood, J., Jefferies, E., 2017. Varieties of semantic cognition revealed through simultaneous decomposition of intrinsic brain connectivity and behaviour. *Neuroimage* 158, 1–11. <https://doi.org/10.1016/j.neuroimage.2017.06.067>

Visser, M., Jefferies, E., Embleton, K. V., Lambon Ralph, M.A., 2012. Both the Middle Temporal Gyrus and the Ventral Anterior Temporal Area Are Crucial for Multimodal Semantic Processing: Distortion-corrected fMRI Evidence for a Double Gradient of Information Convergence in the Temporal Lobes. *J. Cogn. Neurosci.* 24, 1766–1778. https://doi.org/10.1162/jocn_a_00244

Visser, M., Jefferies, E., Lambon Ralph, M.A., 2009. Semantic Processing in the Anterior Temporal Lobes: A Meta-analysis of the Functional Neuroimaging Literature. *J. Cogn. Neurosci.* 22, 1083–1094. <https://doi.org/10.1162/jocn.2009.21309>

Visser, M., Lambon Ralph, M. a, 2011. Differential contributions of bilateral ventral anterior temporal lobe and left anterior superior temporal gyrus to semantic processes. *J. Cogn. Neurosci.* 23, 3121–3131. https://doi.org/10.1162/jocn_a_00007

Wang, X., Peelen, M. V., Han, Z., Caramazza, A., Bi, Y., 2016. The role of vision in the neural representation of unique entities. *Neuropsychologia* 87, 144–156. <https://doi.org/10.1016/j.neuropsychologia.2016.05.007>

Whitfield-Gabrieli, S., Nieto-Castanon, A., 2012. Conn: a functional connectivity toolbox for correlated and anticorrelated brain networks. *Brain Connect.* 2, 125–141. <https://doi.org/10.1089/brain.2012.0073>

Yoder, R.M., Clark, B.J., Taube, J.S., 2011. Origins of landmark encoding in the brain. *Trends Neurosci.* 34, 561–571. <https://doi.org/https://doi.org/10.1016/j.tins.2011.08.004>

Zahn, R., Moll, J., Krueger, F., Huey, E.D., Garrido, G., Grafman, J., 2007. Social concepts are represented in the superior anterior temporal cortex. *Proc. Natl. Acad. Sci.* 104, 6430–6435. <https://doi.org/10.1073/pnas.0607061104>

Zhang, M., Savill, N., Margulies, D.S., Smallwood, J., Jefferies, E., 2019. Distinct individual differences in default mode network connectivity relate to off-task thought and text memory during reading. *Sci. Rep.* 9, 1–13. <https://doi.org/10.1038/s41598-019-52674-9>